MONAZITE ALTERATION IN THE SEARCHLIGHT CONTACT METAMORPHIC AUREOLE, SOUTHERN NEVADA

By

Scott A. Crombie

Thesis

Submitted to the Faculty of the

Graduate School of Vanderbilt University

in partial fulfillment of the requirements

for the degree of

MASTER OF SCIENCE

in

Geology

August, 2006

Nashville, Tennessee

Approved:	Date:
John C. Ayers	07/28/06
Calvin F. Miller	07/28/06

ACKNOWLEDGEMENTS

The past two years have been an exceptional academic and social experience. I would like to thank John Ayers for his guidance and patience, Calvin Miller for his indispensable field knowledge and incomparable campfire cooking. In addition to the academics I have meet many wonderful people at Vanderbilt. I would be remiss if I did not thank my fellow students; Lily Lowery-Clayborn, Dan Perrault, Brook Traynham, and Chris Fisher. I could not have asked to come to Vanderbilt with a better class. In addition thanks go out to the rest of the grad room Nichole, BJ, Ben, Sue thanks for the laughs. Finally I would like to thank Mom and Dad for all their love and support.

LIST OF TABLES

LIST OF FIGURES

TABLE OF CONTENTS

CHAPTER I

INTRODUCTION

Purpose

Monazite is a light rare earth element (LREE) phosphate that readily incorporates Th and U into its crystal structure while excluding Pb making it a prime candidate for geochronology. Recent experiments and field studies (Cetiner et al. 2005, Seydoux-Guillaume et al., 2002, Townsend et al., 2000, Loflin 2002, and others) have shown that hydrothermal alteration may result in complex internal zoning and isotopic exchange causing the Th, U-Pb isotopic system to reset. The resetting of this isotope system will produce variable ages that represent different events in the grains history. In settings where country rocks (such as quartzo-feldspathic gneiss or granites) are less sensitive to hydrothermal alteration (than calcsilicates for example) monazite may be useful as a tracer of fluid infiltration.

The Miocene Searchlight pluton in southeast Nevada (fig. 1) intruded into the >1.7 Ga Mojave supercrustal sequence (characterized by interleaved orthogneiss, paragneiss, leucogranites and minor amphibolite), a Proterozoic augen orthogneiss, and Cretaceous granite without forming a distinct contact aureole. Samples were collected from the three main country rock groups and monazite was separated for Th-Pb and U-Pb dating and compared in relation to proximity with the Searchlight contact and extent of alteration to determine if there is a pattern related to distance from the contact.

Figure 1. Location map of Searchlight and Ireteba plutons in southern Nevada.

Previous Work

Laboratory experiments have been conducted to characterize the cause for monazite growth and recrystallization. Ayers et al. (1999) conducted monazite growth experiments in a piston-cylinder apparatus at 1.0 GPa and 1000°C and concluded that monazite in quartzite would rapidly recrystallize and grow in the presence of H2O (2 wt.%) by Ostwald ripening. Additional experimentation with 2 molal NaCl fluid resulted in slowly growing quartz and no monazite coarsening (Giles, 2000). Seydoux-Guillaume et al. (2002) conducted a series of experiments with natural monazite samples and variable fluid compositions at quartz saturation at 800°C and 700 MPa. In addition, experiments with pure water over a temperature range of 800 – 1200 °C, at 700 MPa with durations ranging from 5 to 60 days were conducted (Seydoux-Guillaume et al. 2002). Pure water experiments showed that even at temperatures as high as 1200 °C dissolution and recrystallization of new monazite was confined to the outermost surface of the grain (Seydoux-Guillaume et al. 2002). Significant overgrowth of newly formed monazite occurred only in the 1000 °C experiments when either CaCl2 or Pb-bearing fluids were present (Seydoux-Guillaume et al. 2002). In the CaCl2 experiment, two zones could be distinguished within the crystal: a core possessing the initial monazite composition and a rim consisting of newly formed monazite produced by dissolution/precipitation, which was enriched in calcium and Pb-free (Seydoux-Guillaume et al. 2002). None of the reaction products contained a detectable Pb diffusion profile. The only resetting mechanism detected involved dissolution/precipitation (Seydoux-Guillaume et al. 2002). The results of these experiments suggest that the extent of dissolution/precipitation of monazite is highly dependent on fluid composition. Other laboratory experiments have

investigated monazite solubility as it relates to fluid pH. Monazite is insoluble in neutral fluids, but is known to be soluble in low pH fluids at low P-T conditions (Ayers, 1991, Wood and Williams-Jones 1994, Cetiner et al. 2005). Single crystal weight loss measurements made in a piston-cylinder apparatus at 1.0 GPa and 1000 °C in H2O ± NaOH ± HCl show that monazite is soluble at both low and high pH (Ayers et al. 2001). The U-shaped solubility curve suggests that monazite solubility is enhanced by REE complexation with hydroxyl ions, thus indicating that both acidic and alkaline fluids have the potential to recrystallize monazite.

Several field studies (McFarlane et al. 2005, Catlos and Cemen 2005, Pyle and Spear 2003, Townsend et al. 2000, Braun et al. 1998) indicate that monazite often undergoes episodic dissolution/precipitation during metamorphic events, and this process of dissolution/precipitation can reset the Th,U-Pb isotope system in the monazite crystal. Various age dating techniques can then be applied to the crystal to relate these replacement zones to specific geologic events. Townsend et al. (2000) identified a bimodal age distribution in monazite from the ~ 66 Ma Ireteba pluton in southeastern Nevada (Kapp et al., 2002). Ion probe Th-Pb dating yielded 60-65 Ma ages for magmatic and some replacement zones in monazite from shallow samples, and crosscutting secondary zones that have a vein like appearance yielded apparent ages as young as mid-Tertiary (Townsend et al. 2000). Monazite from deeper samples yielded a few 55-65 Ma ages for remnant magmatic zones and abundant Miocene ages for replacement zones (~17-18 Ma) (Townsend et al. 2000). The bimodal age distribution was interpreted to represent the dissolution/precipitation of select monazite zones by fluids released during

the emplacement and cooling of the adjacent Miocene Searchlight and Aztec Wash plutons (Townsend et al. 2000).

Other field studies have focused on the use of $\delta^{18}O$ values as a way to trace the origin of fluids that were responsible for dissolution/precipitation in monazite. If in fact the Th,U-Pb isotope systems are being altered by hydrothermal fluids it is not unreasonable to assume that the oxygen isotope system may also be altered. Monazite from samples of Ireteba granite along the Searchlight contact dated by Townsend et al. (2000) were analyzed for oxygen to compare the distribution of age with $\delta^{18}O$ composition (Loflin 2002). Unlike the Th-Pb ages reported for these samples the oxygen isotope analysis shows a unimodal distribution for replacement and primary zones within each sample (Loflin 2002). For example, primary zones in monazites from Ireteba sample IR1 have a mean $\delta^{18}O$ value of 7.79±0.46 (95% conf. limits) ‰, while secondary zones have a mean of 7.39±0.40‰ (Loflin 2002). Because the oxygen isotope composition of monazite did not change significantly during dissolution/precipitation, the Searchlight Ireteba contact zone was likely rock dominated. The low fluid/rock ratio allowed the Ireteba granite to buffer the $\delta^{18}O$ signature of any fluids released by the Searchlight (Loflin 2002). While these studies clearly demonstrate that monazite in the Ireteba granite was recrystallized and reset at the same time as the intrusion of the Searchlight pluton, they do not clearly demonstrate the extent to which hydrothermal fluids were involved or the extent to which the Searchlight intrusion may have altered other country rock in the area.

Geologic Setting

The Searchlight Pluton is exposed in the southern Eldorado and northern most Newberry Mountains, in southeastern Nevada. These ranges are constructed of large west tilted fault blocks that lie in the northern Colorado River Extensional Corridor, a 50 to 100 km wide extensional belt, which underwent peak extension and magmatism ~ 16 to 15 Ma (Faulds et al., 1990). Miocene age volcanic and sedimentary strata are exposed along the western edge of these fault blocks (Bachl et al., 2001). The volcanic rocks range in composition from rhyolite to basalt (Bachl et al., 2001). Basement rocks consist mainly of Proterozoic granites and meta-igneous and meta-sedimentary gneisses intruded by mafic to felsic plutonic rocks that are coeval with the volcanic strata (fig. 2) (Bachl et al., 2001).

The Searchlight pluton is part of a large west dipping block in the foot wall of the Dupont fault (Bachl et al., 2001). The tilting has exposed this pluton in cross section with the shallow levels exposed to the west and the deeper levels of the pluton exposed in the east (Bachl et al., 2001). The upper Searchlight pluton is a fine to medium grained quartz monzonite (63 – 71 wt% SiO_2). The middle Searchlight is a medium grained granite (69 – 78 wt% SiO_2), and the lower Searchlight is a coarse grained quartz monzonite (59- 70 wt% SiO_2) (Bachl et al., 2001). Measurements of crystallization depth by aluminum-in-hornblende barometry suggest an initial depth for the roof of the pluton at 3 km and the floor at 13 km (Bachl et al., 2001). Zircon geochronology documents an approximately two million year history for the pluton with ages ranging from 15.8 Ma to 17.7 Ma (Cates et al., 2003, Miller et al., 2003, Means et al., 2003). The great majority of the pluton, however, appears to have crystallized in the interval 15.8-16.8 Ma. To the

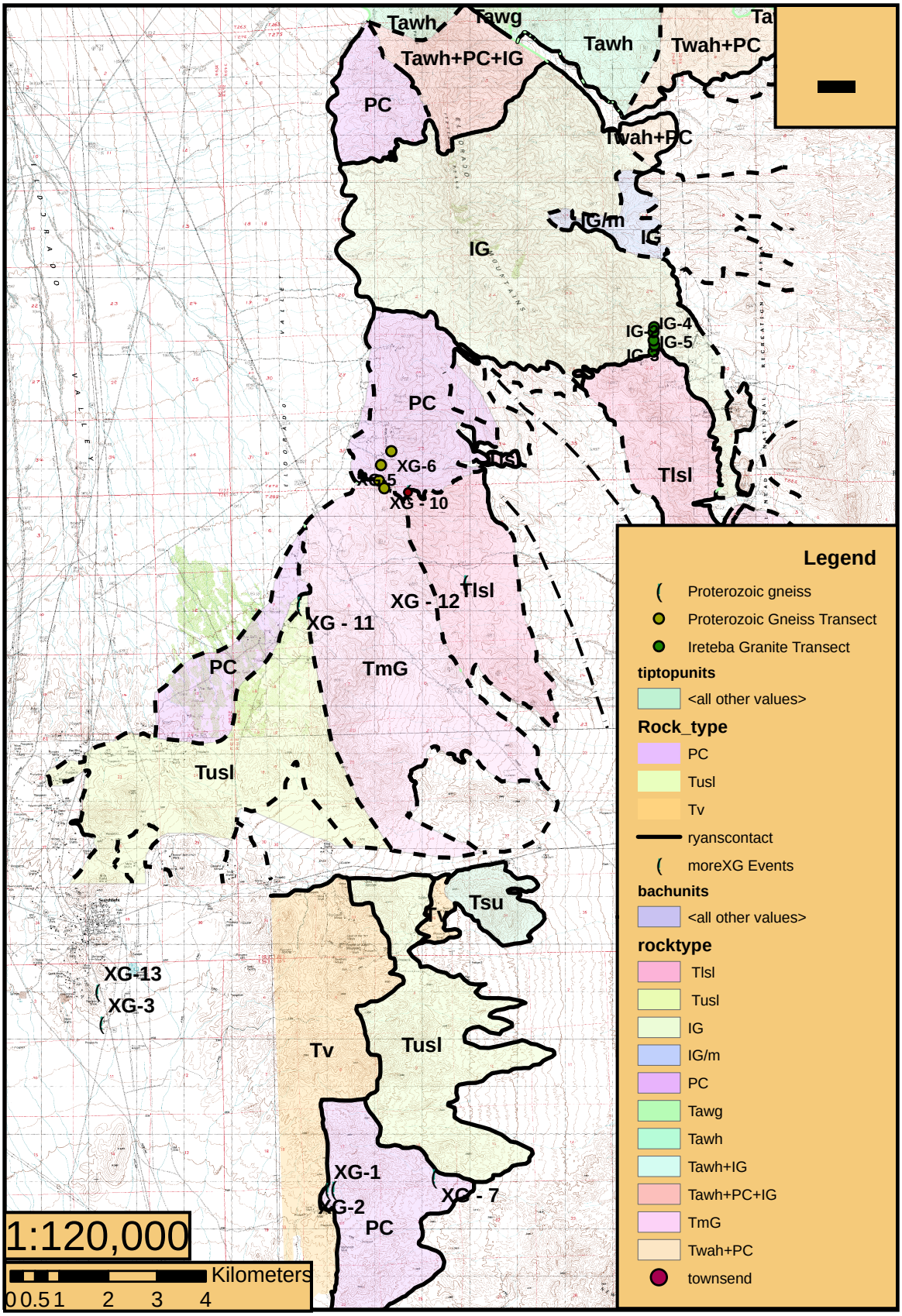

Figure 2. Geologic map of field area

southwest the upper pluton contacts both Proterozoic augen gneiss and Miocene volcanics. Along the northern border of the pluton, from shallow to mid level the margin is characterized by intrusions into Proterozoic gneiss where decimeter to hundred meter long tongues of granitic rock intrude preexisting gneissic fabric (Bachl et al., 2001). In these tongues the magmatic foliation in the granite parallels the preexisting gneissic fabric while in areas without tongues the Searchlight does not display foliation (Bachl et al., 2001). It is likely that the Searchlight exploited planes of weakness in the gneissic fabric to create these tongues, but in general the Proterozoic gneiss behaved rigidly along this margin (Bachl et al., 2001). Deeper portions are bounded by the ~66 Ma Ireteba granite creating a moderately irregular contact, with reentrants of up to 200-300 m, and felsic dikes from the lower unit that penetrate the Ireteba granite up to several hundred meters; however, the contact is razor sharp in outcrop (Bachl et al., 2001). Figure 3 is a schematic cross-section of the pluton after emplacement.

Proterozoic country rocks are of the Mojave province. The original age of the Mojave crust is somewhat debated. No rocks have been dated at > 1.8 Ga, but Nd and Pb isotope compositions suggest involvement of crustal material greater > 2 Ga (Bennett and DePaolo, 1987). This original crust was intruded at 1.73 – 1.76 Ga by gabbroic to granitic magmas (now gneiss), which were then altered and intruded by granites and some gabbros during the 1.70 – 1.72 Ga Ivanpah orogeny (Wooden and Miller, 1990). After peak orogeny the eastern Mojave was intruded by abundant intermediate to felsic magmas between 1.62 and 1.69 Ga (Wooden and Miller, 1990). At 1.40 – 1.45 Ga the eastern Mojave crust was intruded by a moderate volume of granitic, with some mafic, magma forming part of the ca. 1.4 Ga “anorogenic” granite belt that transects North

America (Miller and Wooden, 1993). The last Proterozoic event recorded in the eastern Mojave was the intrusion of diabase dikes and sills at 1.1 Ga (Hammond and Wooden, 1990). The region was part of a passive continental margin from the Cambrian through Triassic (Stone et al., 1983).

The current Proterozoic exposures in the Searchlight area consist of three main lithologies. The southern roof area (see fig. 2) is chiefly augen orthogneiss with sutured quartz grains, highly altered plagioclase, K-spar porphyroblasts with quartz pressure shadows, muscovite, chlorite, opaques, zircon, apatite and cross cutting epidote rich veins. The northern roof zone and wall zone (see fig. 2) are a complex zone of biotite and sometimes garnet rich paragneiss, interleaved with orthogneiss, leucogranites that can be garnet rich, and minor amphibolites.

The ~66 Ma Ireteba pluton also experienced tilting during Miocene extension (Kapp et al., 2002). The current exposures of the pluton were ~5-13 km deep at 16 Ma. Like the Searchlight the current exposures represent a cross section with the shallowest levels to the west and deeper levels to the east (Falkner et al. 1995; Patrick and Miller 1997; Bachl et al. 2001). The Ireteba is a two-mica granite composed of plagioclase, quartz, K-feldspar, biotite, muscovite, and accessory minerals (Kapp et al. 2002). Along the southern margin of the pluton the shallow levels are in contact with Proterozoic gneiss and the deeper portions contact the 16.9 Ma Lower Searchlight quartz monzonite, while the northern border of the pluton is in contact with the 15.8 to 15.6 Ma Aztec Wash pluton (Cates et al., 2003). The Ireteba pluton is generally undeformed. However, the southeastern part of the pluton has a weak to strong linear ductile fabric, and a band of highly deformed granite extends southward from the southeast corner of the main mass,

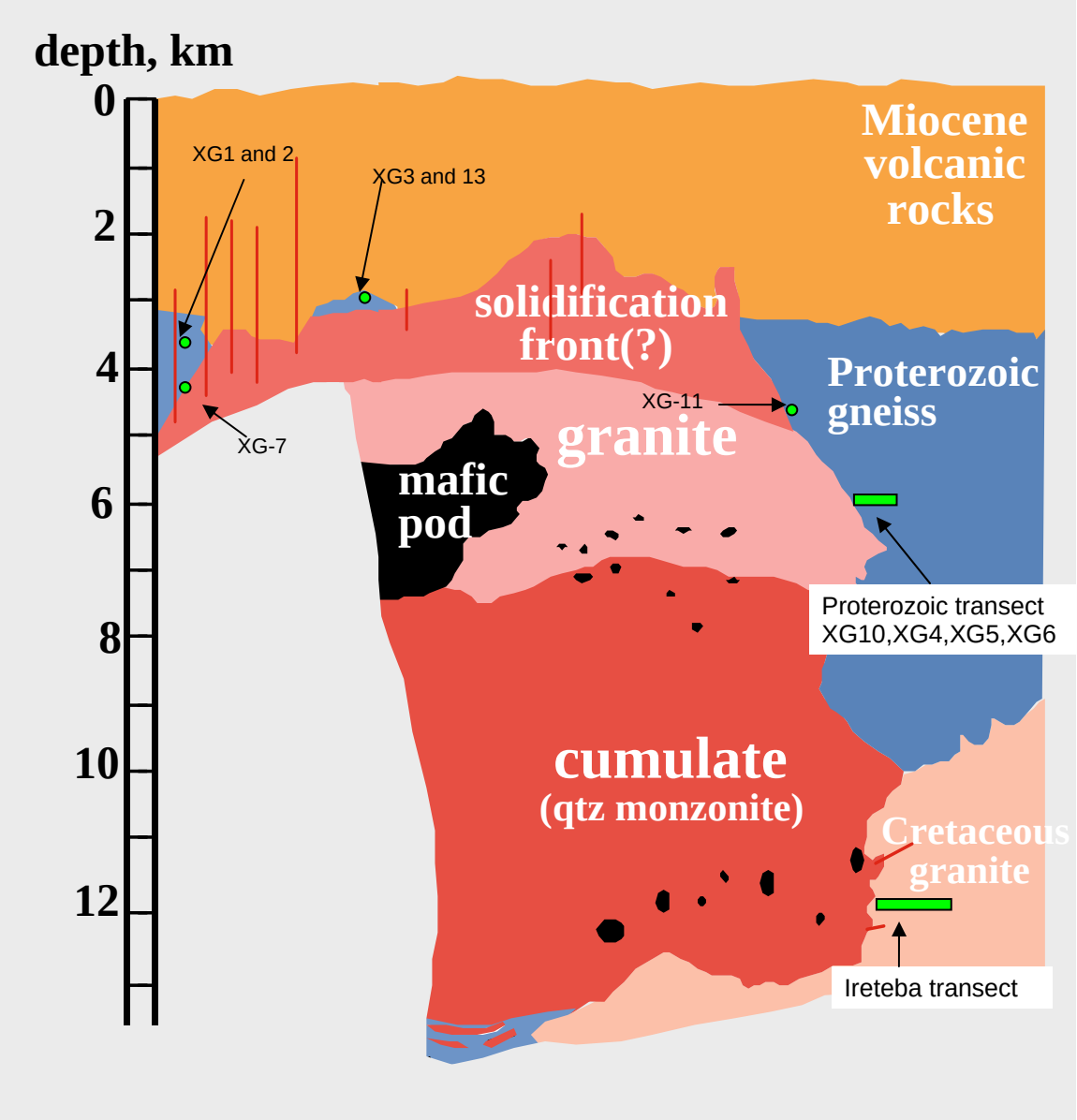

Figure 3. Schematic cross section, with no vertical exaggeration, of the Searchlight pluton after emplacement. (from Bachl et al., 2001). Sample locations for this study are located in green and labeled by sample number or transect.

east of the Searchlight pluton, and underlies the east dipping Dupont fault (see fig. 2) (Kapp et al., 2001).

Sample description

The Ireteba samples are all leucogranites with a distinct foliation. Samples IG-1, IG-2, IG-3, and IG-5 are very similar in modal mineral abundance and texture. They contain 15-20% K-feldspar, 35-45 % plagioclase feldspar, 30-35 % quartz, 1 - 5 % biotite + muscovite, and accessory opaques, zircon, monazite, and apatite. All are well foliated with large phenocrysts (up to 1.5 cm in IG-1) of potassium feldspar and smaller phenocrysts of plagioclase feldspar and sutured quartz in a medium grained matrix of feldspar and quartz. The foliation is the result of ductile deformation. The area these samples were collected from has a well defined planer fabric dipping to the west that is shared by the Searchlight plutons lower unit (Townsend et al., 2000). Sample IG-4 is different in that it lacks large phenocrysts and appears to be a weakly foliated equigranular mass of 15 % K-feldspar, 45% plagioclase feldspar and 30% quartz with 5% biotite + muscovite in smaller crystals. In addition, the sample contains large (~2 mm) embayed garnet crystals.

While the lithology of the Proterozoic wall zone rocks is highly variable sample collection focused on those rocks most likely to contain monazite. Samples XG-4, XG-6, and XG-9 are all peraluminous biotite paragneiss and consist of 10 to 20% K-feldspar, 15 to 20 % biotite, 40 to 50 % plagioclase feldspar, and 20 to 30 % quartz with opaques, garnet, apatite, zircon, and monazite as accessory minerals. XG-10 is also a peraluminous biotite paragneiss but contains more K-feldspar than the other samples, 30 to 45% K-

feldspar, 30 to 40 % biotite, 10 to 20% plagioclase feldspar, and 10 to 20% quartz. In general K-feldspars occur as large (slightly to highly altered) porphyroblasts surrounded by bands of small K-feldspar, plagioclase feldspar, and sutured quartz. Biotite occurs in bands and has opaques and garnet associated with it. Biotite also occurs as inclusions in many of the feldspars. Sample XG-5 is a weekly foliated leucogranite containing ~45 % K-feldspar, 30 % quartz, 20 % plagioclase feldspar, and 5% garnet porphyroblasts partially altered to chlorite. Accessory minerals include opaques, zircons, and apatite. Sample XG-12 (collected from a large country rock block in the lower Searchlight unit) is a quartzo-feldspathic biotite gneiss similar in mineral abundance and fabric to the wall zone gneisses. Samples XG-4 and XG-5 are closest to the contact with the Searchlight, which may explain why they have the weakest foliation (overprinted during contact metamorphism).

Sample XG-11 (collected in the northern roof zone) is a mylonitic quartzo-feldspathic biotite gneiss with ~10 % biotite, 30% quartz, 30% K-feldspar, 30% plagioclase feldspar, and accessory opaques, zircon, and monazite. Quartz shows undulatory extinction and mainly occurs with feldspars in leucocratic bands. These bands surround highly sericitized K-feldspar porphyroclasts.

Samples of Proterozoic rocks collected from the southern portion of the roof zone (XG-1, XG-2, XG-3, and XG-13) are all augen orthogneisses with large, highly altered feldspar porphyroblasts (augens) and bands of quartz with undulatory extinction and feldspars. The large porphyroblasts are almost entirely altered to muscovite, epidote, and chlorite. Opaque minerals commonly occur with chlorite crystals. Accessory minerals include zircon, hematite, and apatite. Sample XG-1 is the least altered of all the samples

with some large plagioclase augen nearly unaltered and less epidote and chlorite than the other samples from this area. XG-3 contains epidote-filled fractures and abundant opaques including hematite associated with the breakdown of biotite, suggesting alteration by an oxidizing fluid. XG-13 is the most altered of the samples with large bands of chlorite almost entirely broken down to opaques and hematite and chlorite filling in cracks in plagioclase grains. Based on the degree of sericitization of plagioclase, alteration of biotite and K-feldspar and the abundance of hydrothermal veins, the intensity of hydrothermal alteration increases in the order XG-1 < XG-2 < XG-3 < XG-13.

Sample XG-7 (collected from the southern roof zone) is a intrusive foliated andesitic porphyry with groundmass of 75% plagioclase feldspar, 20% K-feldspar, 5% quartz and accessory amphibole, opaques, epidote, and zircon. Quartz and K-feldspars occur in leucocratic bands around zones of equigranular, twinned plagioclase and large plagioclase feldspar phenocrysts that are highly altered to epidote. Amphiboles are rare and almost entirely altered.

CHAPTER II

METHODS

Samples of the Proterozoic gneiss were collected along a 0.5 km transect northward from the northern margin of the Searchlight pluton into the country rock, from a large block located in the lower Searchlight zone, and from the western margin of the Searchlight pluton near the roof area. Five samples of the Ireteba granite were collected in a 0.9 km north trending transect from the lower Searchlight - Ireteba contact.

Hand samples were cut into 1 inch thick slabs using a Target 16 inch rock saw. One slab from each sample was chosen to cut billets for standard petrographic thin sections. Another slab was pulverized in a shatter box to provide powder for whole rock major and trace element analysis. Oxygen isotope analysis of whole rock powders of samples from the two transects were performed by Actlabs. Whole rock samples from the Ireteba granite transect were analyzed by Actlabs for hydrogen isotopes as well. Whole rock compositional data are presented in Table 3. The remainder of the hand sample was used for mineral separation.

Monazite was separated from hand samples using standard mineral separation techniques. Equipment included (in order of use) jaw crusher, rock pulverizer, water table, heavy liquids, and Franz magnetic separator. Monazite was then hand picked and mounted in 1 inch diameter epoxy rounds with 554 and 44069 monazite geochronology standards and Brazil monazite trace element standard. The epoxy mounts were polished, carbon coated, and then imaged on the Hitachi S-4200 Scanning Electron Microscope

(SEM) at Vanderbilt University. Grains were identified using the SEM's Energy Dispersive Spectrometer, and Back Scattered Electron (BSE) images were collected of each grain. BSE images show micrometer scale differences in brightness that correspond to changes in mean atomic number (composition). Based on these images grains were chosen for analysis by Electron Microprobe (EMP) and Laser Ablation-Inductively Coupled Plasma-Mass Spectrometry (LA-ICP-MS).

Major element and trace element concentrations, and Th-U-Pb chemical dates, of monazite were measured at Rensselaer Polytechnic Institute (RPI) using a Cameca SX-100 electron microprobe. Additional major element and trace element concentrations were collected at University of Tennessee Knoxville on a Cameca SX-50 electron microprobe. The carbon coated epoxy mounts were placed in the Cameca SX-100 instrument and analyzed at 15 kev and 100 nA with a beam width of 5um. BSE images were used to locate spots for analysis. Th-U-Pb chemical ages for monazite are presented in weighted-histograms. Each analysis is represented by a Gaussian curve characterized by the mean and standard deviation of the age measurement. A weighted histogram representation is then obtained by summing all of the Gaussian curves for a sample (Montel 1996). Measured trace element and major element concentrations in monazite are compiled in appendix A. Column conditions used on the Cameca SX-50 microprobe were 20 kev, 40 nA, 3um beam width. Major element and trace element data from this analytical session are compiled in appendix B.

LA-ICP-MS analysis was conducted at Vanderbilt University with a Perkin Elmer 6100 DRC ICP-MS coupled with a New Wave/Merchantek 213 nm Nd:YAG laser, and a mixture of He and Ar carrier gas. He carrier gas was flushed into the ablation cell and

admixed with nebulizer argon ~ 30 cm behind the ablation cell. This mixture was then transported to the ICP-MS. Before each analysis session the laser was allowed to warm up by firing at low power for an hour. NIST-610 glass was used to optimize the instrument. Analytes for all sessions include ^{40}P, ^{139}La, ^{204}Pb, ^{206}Pb, ^{207}Pb, ^{208}Pb, ^{232}Th, ^{238}U, and ^{248}ThO. During the optimization process the laser was fired at analysis settings (5 Hz, 80% power and a 30 um spot size) and the real time signal was monitored so that the rf-power, lens voltage, and nebulizer flow could be adjusted during ablation to increase sensitivity for each analyte. In addition, these parameters were adjusted to keep the ratio of Th/ThO lower than 0.5%. Optimal settings for the sensitivity and dwell times for each analyte are listed in Table 1. The 1 inch epoxy mounts were placed in the ablation chamber, and BSE images were used to choose analysis locations. Unknown data was collected in groups of five analyses bracketed by analysis of external standards (554 for 208Pb/232Th and 44069 for 206Pb/238U and 207Pb/235U). Two analyses of each standard were collected between groups of unknowns. After every fourteen analyses NIST-610 was analyzed again. Each analysis lasted for 100 seconds. During the first 30 seconds the laser was not firing so a background signal could be collected. Ablation actually lasted for 70 seconds. Raw data was then transferred to the GLITTER software package for reduction. GLITTER calculates the relevant isotopic ratios and displays them as time-resolved intensity traces (Van Achterbergh et al., 2001). The time-resolved signals were then inspected and the most stable portions of the signal were selected for integration. After reviewing all analyses, isotope ratios and errors were exported to Microsoft Excel and the Isoplot add-in (Ludwig, 2001) was used to generate concordia plots and probability density histograms.

Table 1. LA-ICP-MS operating conditions and data acquisition parameters

ICP-MS		gas flow		Laser	
Lens voltage	5 v	Plasma	15 L/min	wavelength	213 nm
rf-power	1400 v	Auxiliary	1 L/min	repetition rate	5 Hz
analog stage voltage	-2150 v	Nebulizer	0.78 L/min	spot size	30 um
pulse stage voltage	1200 v			pulse energy density on sample	~11 j/cm^2

Data acquisition parameters

protocol	time resolved analysis
scanning mode	peak hopping
detector mode	duel
Isotopes determined	^{40}P, ^{139}La, ^{204}Pb, ^{206}Pb, ^{207}Pb, ^{208}Pb, ^{232}Th, ^{238}U, ^{248}ThO
dwell time per isotope	10, 10, 10, 20, 20, 10, 10, 10, 10, ms respectively
Data acquisition time	70 s
background acquisition time	30 s

Monazite Standards

554	45±1 Ma	used for Th-Pb dating
44069	424.86±0.5 Ma	used for U-Pb dating

CHAPTER III

RESULTS

Whole Rock Chemistry

Proterozoic samples are strongly peraluminous with silica ranging from 60 to 75%, and they include high and low K2O variants (Table 3). Sample XG-2 is roughly 2.3 times as rich in CaO compared to the other samples. Proterozoic and Ireteba samples plot within the volcanic arc and continental granite field on Pearce diagrams (Fig. 4 and 5). Proterozoic sample Spider plots normalized to primitive mantle display an arc signature. However, XG-5 (Proterozoic granite) has a large positive Eu anomaly (Fig. 6). Samples have ~200 times chondritic LREE, and range from about 5 times to 50 times chondritic concentrations of HREE (Fig. 7).

The Ireteba granite is a strongly peraluminous granite with silica ranging from 72 to 75 wt% (table 3). Major and trace element concentrations plotted on discrimination diagrams agree with data from Kapp et al. 2002 showing that compatible elements (Ca, Mg, Fe, Ti, Al, Sr, Ba, LREE) decrease and incompatible elements (Rb, K), though scattered, increase with increasing SiO2 (Fig. 8). Ireteba granites plot within the volcanic arc field on Pearce diagrams (Fig. 4 and 5). Generally, the samples have ~100 times chondritic LREE, are depleted in HREE (1.5 to 3.6 times chondritic values), and lack Eu anomalies (Fig. 7). However, IG-4 has a negative Eu anomaly and a higher concentration of HREE (7 times chondritic values).

Whole rock oxides from two samples of Ireteba granite were used to construct an isocon plot (Fig. 9). An isocon plot compares the concentration of various components between an altered and an unaltered sample of rock (Winter 2001). Any line that connects the origin with a point representing the concentration of any single component in both rocks can be called an "isocon" (line of constant concentration) (Winter 2001). An isocon with a slope of one corresponds to equal concentration in the altered and unaltered rocks (Winter 2001). Components that plot above the isocon with slope one are said to be gained in the altered rock and those that plot below are said to be lost (Winter 2001). For the Ireteba granite samples IG-1, a sample at the Searchlight contact, was chosen as the altered rock and IG-5, a sample 0.46 km from the Searchlight contact, was selected to represent unaltered rock. All major element oxides from table 3 are plotted in Figure 9. All the major oxides except K2O and Na2O fall with in two sigma error of the isocon with a slope of one. K2O plots above the isocon indicating a gain in concentration, and Na2O plots below the isocon indicating a loss in concentration. Potassium metasomatism is a common occurrence in the innermost aureoles of calcalkaline intrusions. The replacement of plagioclase feldspar by potassium feldspar (the sericitization observed in thin sections of these samples) can account for the observed change in bulk rock composition. Due to the variability in composition of the protoliths of the Proterozoic gneiss samples an isocon investigation was not possible.

Table 2. Whole Rock Major and Trace Element Composition of samples

	Ireteba Granite					Proterozoic Gneiss								LSL	Porphyry
Sample	IG-1	IG-2	IG-3	IG-4	IG-5	XG-2	XG-4	XG-5	XG-6	XG-9	XG-10	XG-11	XG-12	LSG-1	XG-7
Yield %	14.4	14.8	13.7	14.6	14.3	--	14.4	14.7	14.2	--	13.6	--	--	--	--
$d^{18}O$[d]	8.9	8.1	9.5	8.9	8.5	--	12.4	10.3	10.7	--	8.3	--	--	--	--
SiO2[a]	75.29	75.14	74.40	72.51	75.00	67.70	75.00	73.38	73.07	66.28	63.55	71.21	61.58	66.68	59.63
Al2O3[a]	13.83	14.23	14.85	16.15	14.49	13.83	12.90	14.68	14.71	13.76	16.66	14.25	17.76	17.18	16.76
Fe2O3[a,b]	0.87	0.91	0.90	0.85	0.90	4.64	4.04	0.61	3.49	8.28	7.75	3.81	6.20	2.90	6.92
MnO[a]	0.01	0.02	0.02	0.06	0.06	0.08	0.14	0.02	0.04	0.14	0.09	0.03	0.06	0.05	0.12
MgO[a]	0.17	0.19	0.18	0.13	0.14	1.83	0.93	0.17	0.77	2.75	2.53	1.49	2.30	1.12	3.36
CaO[a]	1.37	1.55	1.65	0.91	1.46	4.82	2.11	0.69	1.42	1.79	0.24	1.22	2.06	2.77	5.36
Na2O[a]	3.67	4.17	4.42	4.44	4.36	4.08	2.55	2.40	2.93	2.68	1.27	2.63	3.20	4.37	4.27
K2O[a]	4.66	3.66	3.46	4.85	3.49	2.00	2.01	7.93	3.00	3.22	6.87	4.86	5.82	4.19	2.08
TiO2[a]	0.07	0.08	0.06	0.05	0.05	0.76	0.26	0.01	0.48	1.03	1.00	0.45	0.93	0.54	1.04
P2O5[a]	0.05	0.05	0.05	0.05	0.04	0.26	0.05	0.09	0.08	0.07	0.04	0.06	0.08	0.19	0.46
LOI	0.52	0.55	0.51	0.44	0.73	2.6	0.9	0.37	1.06	0.99	1.76	0.79	0.74	0.79	1.08
Total[c]	99.84	99.89	99.74	99.78	99.21	99.54	99.73	99.73	99.9	100	99.23	99.53	99.53	99.6	99.9
Sc	< 1	2	2	4	2	9	21	3	5	21	18	16	16	5	13
Be	2	1	1	1	1	1	< 1	1	< 1	2	4	5	4	3	2
V	11	< 5	6	< 5	< 5	71	11	< 5	39	125	119	56	115	39	104
Cr	< 20	< 20	< 20	< 20	< 20	40	< 20	< 20	30	80	90	40	80	< 20	80
Co	< 1	< 1	< 1	< 1	< 1	7	4	< 1	5	15	14	5	8	5	14
Ni	< 20	< 20	< 20	< 20	< 20	< 20	< 20	< 20	< 20	40	30	< 20	20	< 20	40
Cu	< 10	< 10	< 10	50	< 10	< 10	< 10	< 10	< 10	< 10	< 10	< 10	< 10	< 10	30
Zn	< 30	< 30	< 30	60	30	< 30	< 30	< 30	50	70	60	< 30	30	< 30	60
Ga	13	13	13	16	14	15	13	10	15	17	26	14	17	16	17
Ge	1.1	1.2	1	1.4	1.2	1.9	1.7	1.6	1.9	1.8	1.6	1.3	1.7	1.2	1.2
As	< 5	< 5	< 5	< 5	< 5	< 5	< 5	< 5	< 5	< 5	< 5	< 5	< 5	< 5	< 5
Rb	73	55	64	111	79	32	68	135	72	153	138	133	159	88	44
Sr	511	492	479	162	383	502	224	267	200	153	136	248	483	600	775
Y	5.2	3.8	6	14.7	5.8	11.9	78.4	10.5	12.4	49.1	25.4	49.5	46.8	17.7	16.6
Zr	62	62	43	31	36	159	391	22	156	297	253	230	293	227	179
Nb	1.9	2.7	2.8	5.7	3.6	10.5	8	0.7	9.5	15.5	18	8.8	12.3	15.2	10.6
Mo	< 2	< 2	< 2	< 2	< 2	< 2	< 2	< 2	< 2	< 2	< 2	< 2	< 2	< 2	< 2
Ag	< 0.5	< 0.5	< 0.5	< 0.5	< 0.5	< 0.5	< 0.5	< 0.5	< 0.5	< 0.5	< 0.5	< 0.5	< 0.5	< 0.5	< 0.5
In	< 0.1	< 0.1	< 0.1	< 0.1	< 0.1	< 0.1	< 0.1	< 0.1	< 0.1	< 0.1	< 0.1	< 0.1	< 0.1	< 0.1	< 0.1
Sn	< 1	< 1	< 1	< 1	< 1	< 1	< 1	< 1	< 1	2	< 1	< 1	< 1	< 1	< 1
Sb	0.9	0.9	0.9	1	0.7	1.1	0.7	0.8	1.3	0.9	1.1	0.6	1	1.2	1
Cs	0.4	0.4	0.4	0.5	0.4	0.3	1.1	3.8	1.3	3.7	3.7	4	3.8	1.1	1
Ba	1406	1413	1218	593	1099	555	517	1698	793	418	1306	1182	2310	1297	1213
La	16	12.2	11.7	10.6	6.46	58.6	62.6	24.9	52.8	69.7	44.5	51.7	50.6	26.1	34.2
Ce	30	23.3	23	22.8	12.4	110	131	33.9	104	146	87.7	101	99.5	48.3	77.5
Pr	3.36	2.66	2.69	2.89	1.43	11.5	16.2	2.9	11.9	17.3	10.4	11.6	11.7	5.52	9.76
Nd	10.7	9.24	9.21	11.3	4.78	36.7	58.9	8.02	41.1	61.4	36	40	39.6	19.1	35
Sm	1.99	1.51	1.72	2.57	1.08	5.22	12	0.92	6.2	11.1	5.88	7.08	6.85	3.67	6.21
Eu	0.52	0.528	0.529	0.35	0.364	1.44	1.84	1.79	2.12	1.68	1.36	1.41	1.92	1.44	2.03
Gd	1.43	1.18	1.47	2.51	0.97	4.09	12.5	0.74	4.89	10.1	5.74	7	6.29	3.37	5.25
Tb	0.19	0.14	0.2	0.4	0.16	0.49	2.11	0.17	0.61	1.5	0.94	1.28	1.06	0.51	0.67
Dy	0.93	0.66	1.08	2.32	0.92	2.4	13.1	1.36	2.63	8.35	5.01	8.16	6.93	2.9	3.24
Ho	0.17	0.12	0.2	0.46	0.18	0.41	2.84	0.33	0.41	1.67	0.9	1.76	1.58	0.59	0.6
Er	0.5	0.37	0.55	1.38	0.57	1.1	9.15	1.09	1	5.03	2.39	5.48	4.98	1.77	1.6
Tm	0.077	0.058	0.083	0.224	0.095	0.157	1.46	0.174	0.119	0.735	0.313	0.841	0.815	0.27	0.22
Yb	0.51	0.44	0.54	1.45	0.69	0.99	9.42	1.11	0.65	4.61	1.84	5.38	5.29	1.7	1.37
Lu	0.078	0.071	0.08	0.212	0.109	0.144	1.36	0.149	0.089	0.688	0.265	0.767	0.774	0.247	0.188
Hf	2.2	2.1	1.5	1.6	1.6	4.3	11.3	1.1	4.6	8.4	7.4	6.8	8.6	5.9	4.5
Ta	0.32	0.1	0.11	0.14	0.15	0.77	0.39	0.19	0.68	0.95	0.93	0.49	0.67	0.93	0.49
W	< 0.5	< 0.5	1.4	< 0.5	< 0.5	< 0.5	< 0.5	< 0.5	0.5	0.5	0.7	1.2	4.4	0.9	< 0.5
Tl	0.32	0.29	0.34	0.56	0.47	0.19	0.38	0.74	0.44	1.01	0.89	0.6	0.99	0.53	0.34
Pb	22	22	20	26	27	10	15	43	20	14	11	6	50	18	15
Bi	< 0.1	< 0.1	< 0.1	0.1	< 0.1	< 0.1	< 0.1	< 0.1	< 0.1	< 0.1	< 0.1	< 0.1	< 0.1	0.2	< 0.1
Th	7.29	3.17	2.91	5.47	1.16	10.3	17.3	1.1	15.4	20	12.2	16	17.4	10.4	0.74
U	0.95	0.51	0.23	0.38	0.21	0.48	3.01	0.52	0.85	2.25	1.03	1.68	1.81	1.49	0.19

[a] oxides in weight percent, normalized to 100% total.

[b] Total Fe as Fe_2O_3.

[c] Total oxides plus LOI prior to normalization.

[d] delta ^{18}O (SMOW) parts per mill

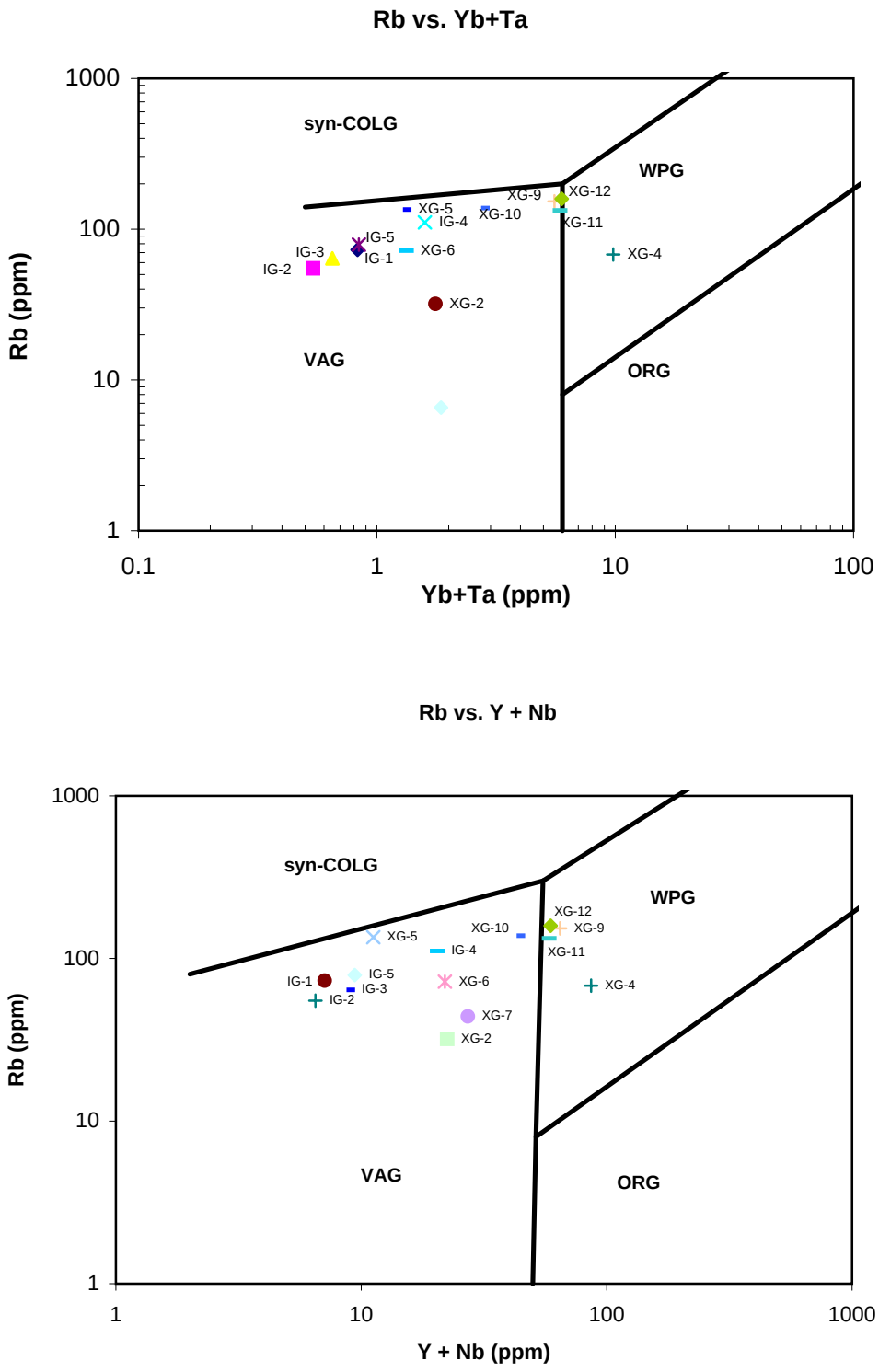

Figure 4. Discrimination diagrams for granitic rocks (after Pearce et al., 1984) showing fields of syn-collisional granites (syn-COLG), with in plate granites (WPG), volcanic-arc granites (VAG), and ocean-ridge granites (ORG).

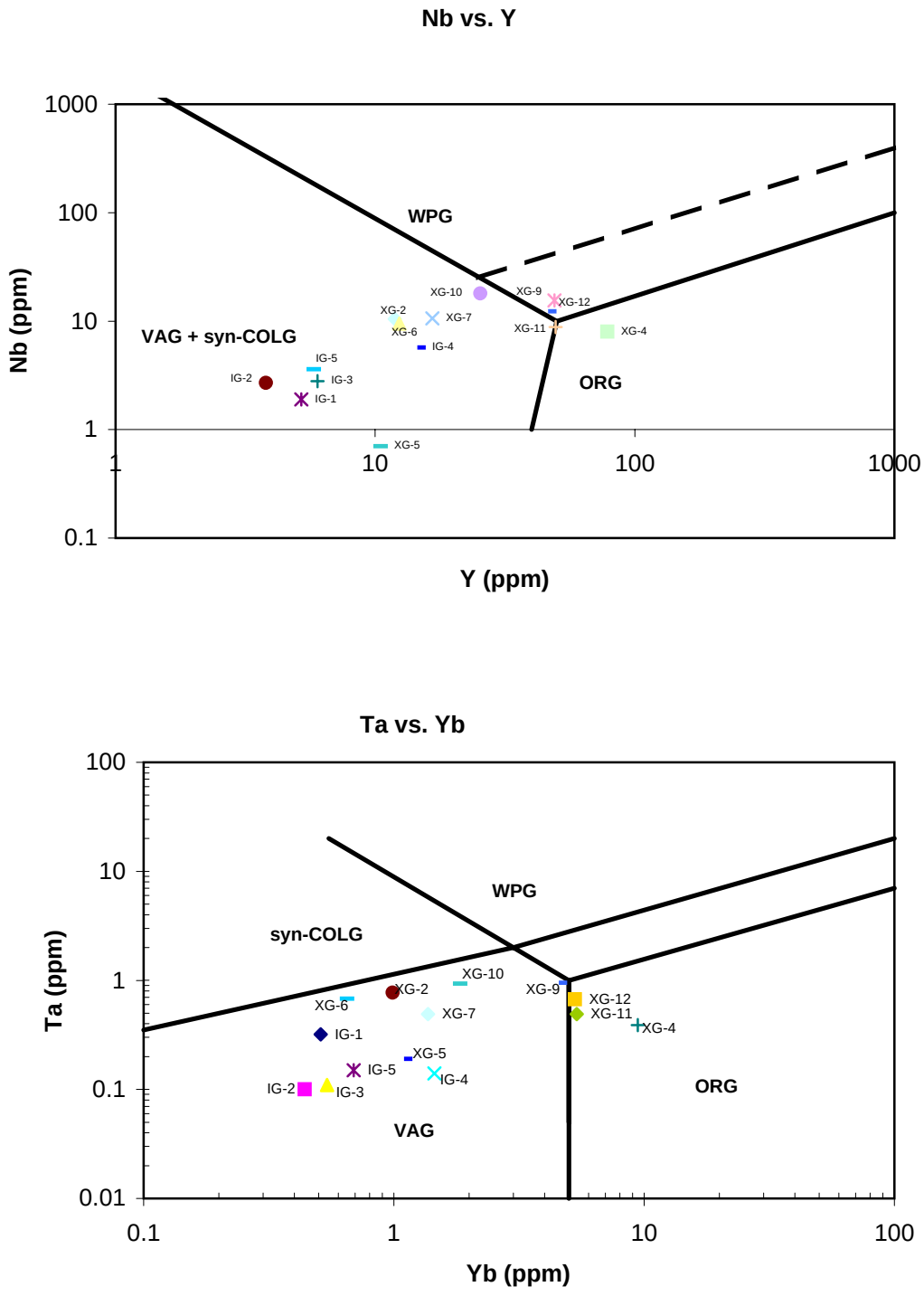

Figure 5. Discrimination diagrams for granitic rocks (after Pearce et al., 1984) showing fields of syn-collisional granites (syn-COLG), with in plate granites (WPG), volcanic-arc granites (VAG), and ocean-ridge granites (ORG).

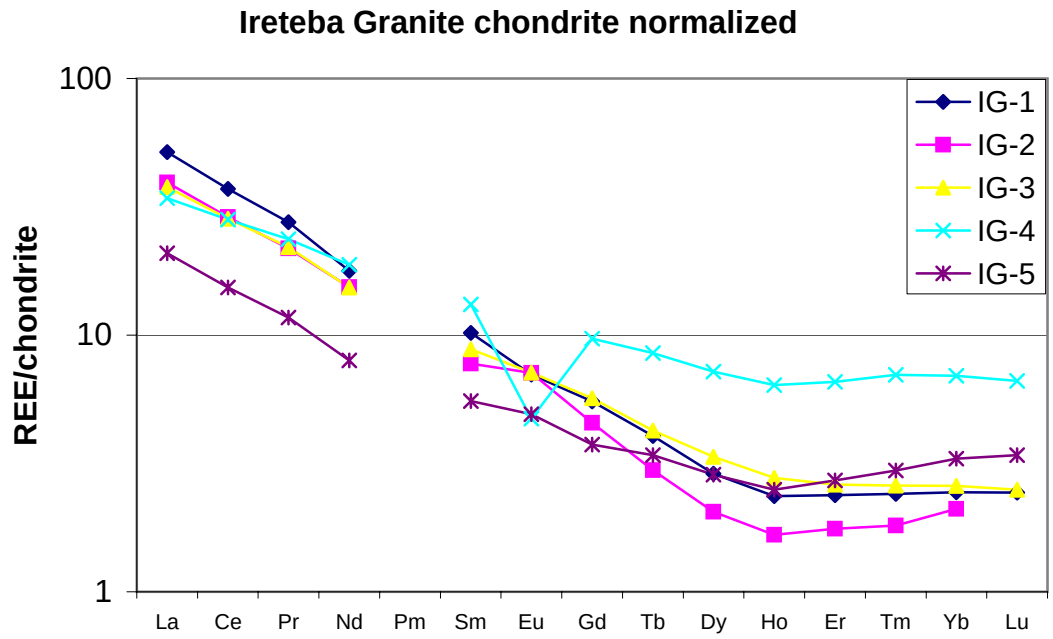

(a)

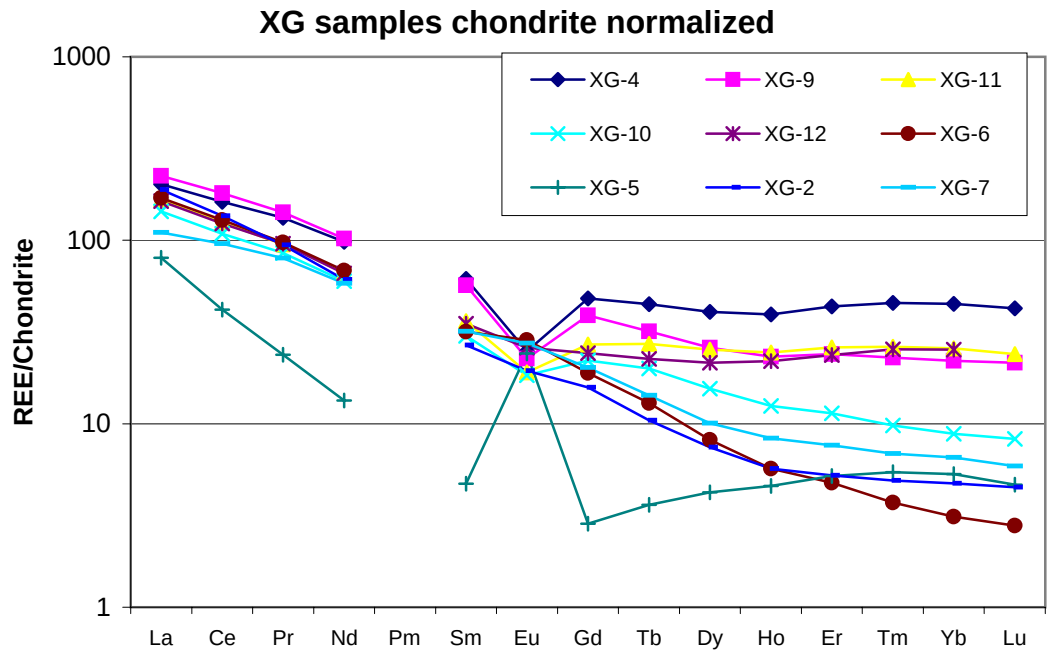

(b)

Figure 6. Chondrite normalized spider diagrams of (a) Ireteba granite and (b) Proterozoic gneiss with XG-7 a porphyritic andesite. Chondrite values from Taylor and McLennan (1985).

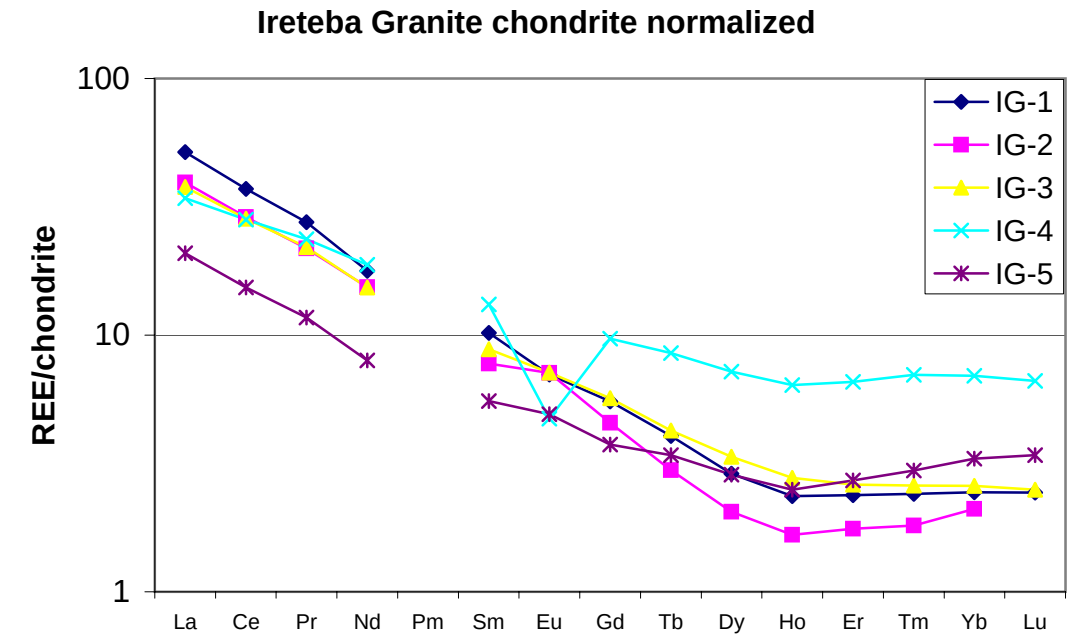

(a)

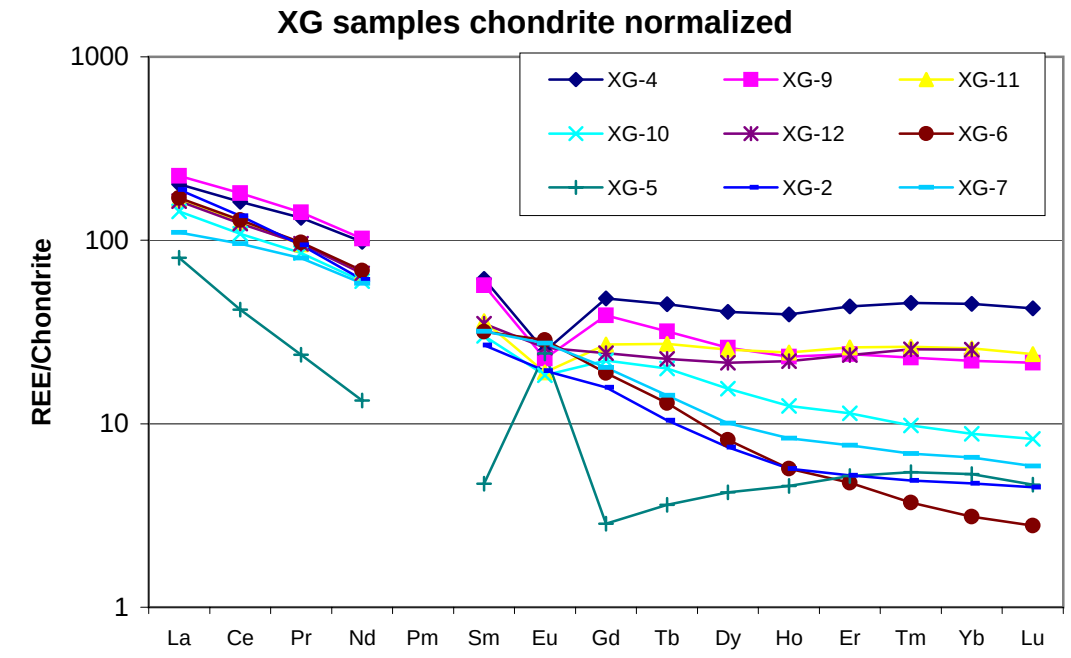

(b)

Figure 7. Chondrite normalized spider diagrams of (a) Ireteba granite and (b) Proterozoic gneiss with XG-7 a porphyritic andesite. Chondrite values from Taylor and McLennan (1985).

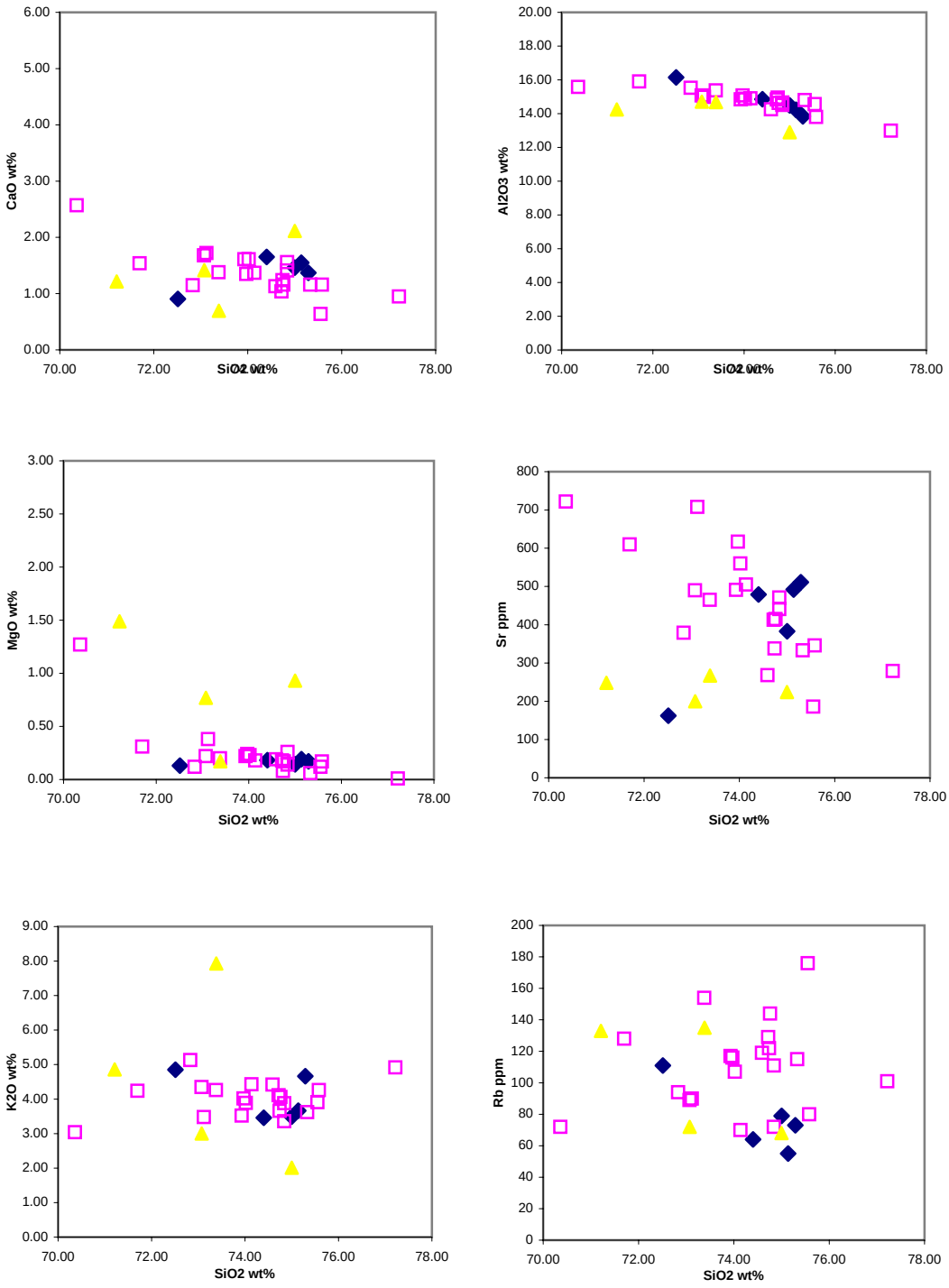

Figure 8. Variation of selected elements versus SiO2. a, CaO; b, AL2O3; c, MgO; d, Sr; e, K2O; f, Rb. Closed diamond symbols represent the five samples of Ireteba granite collected for isotope analysis in this study while the open symbols represent data from Ireteba granite presented in Kapp et al., 2001. Triangles represent Proterozoic gneiss samples from this study.

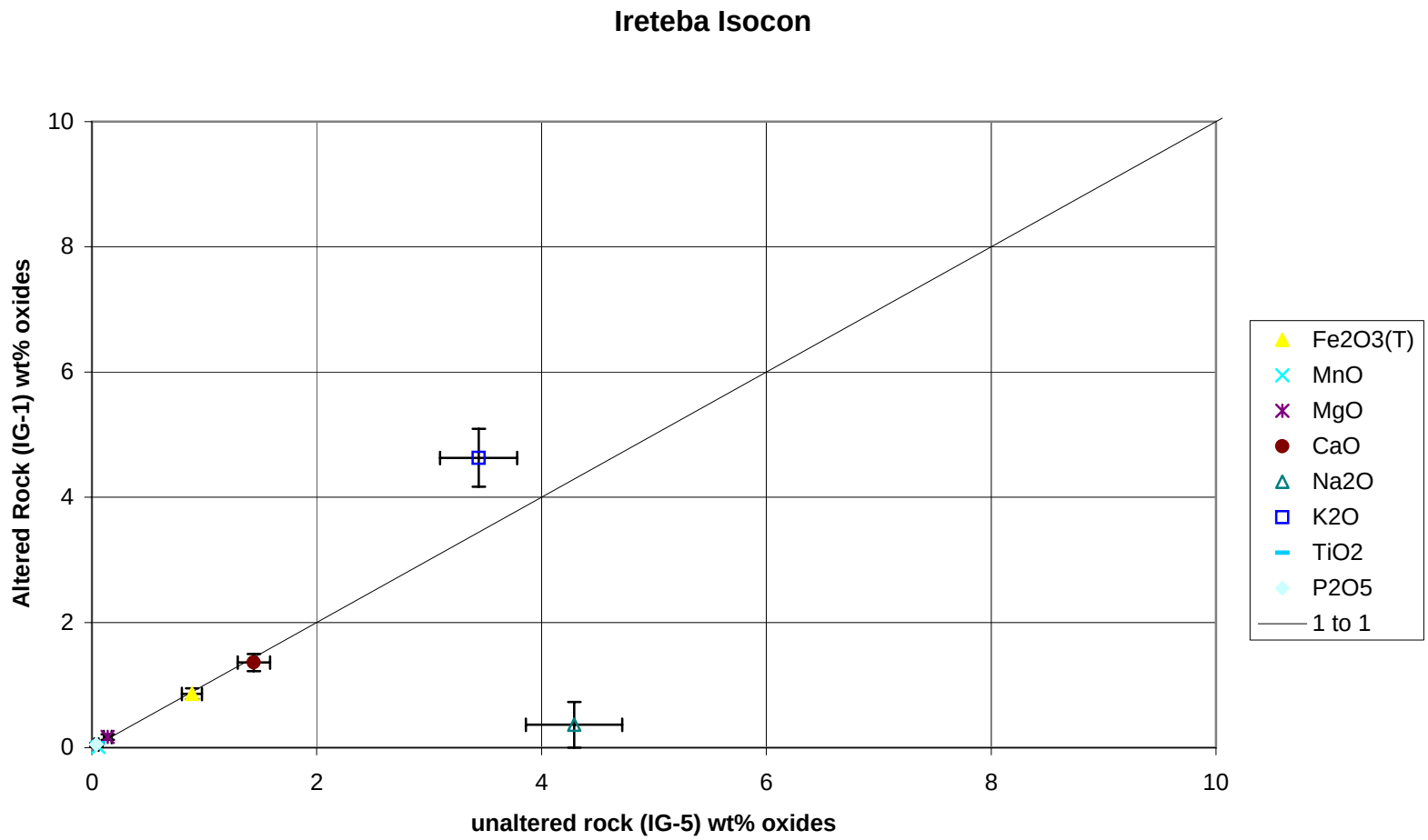

Figure 9. Isocon plot (as in Winter 2001) of Ireteba granite concentrations in wt% with two sigma error bars. The black line with slope of one represents a line of constant concentration. Al2O3 and SiO2 are with in error of the line of constant concentration at x=14.27, y=13.74 and x=73.86, y=74.78 respectively. MgO, TiO2, P2O5 are all with in error of the line of constant concentration.

Whole rock Isotope Analysis

If hydrothermal alteration of monazite caused the partial resetting of the U,Th-Pb isotopic clock within monazite grains it is likely that the same alteration may have affected oxygen isotope and hydrogen isotope compositions of the host rocks as well. The magnitude of the shift in $\delta^{18}O$ and δD would depend on the fluid/rock ratio, temperature, and the isotopic compositions of fluid and rock. Any shift in $\delta^{18}O$ or δD might be used as a tracer to determine the origin of the hydrothermal fluid. To this end whole rock powders from the Proterozoic gneiss transect were sent to Actlabs for oxygen isotope analysis. Whole rock powders from the Ireteba granite transect were also sent to Actlabs for both oxygen and hydrogen isotope analysis.

Whole rock δ18O values for the four samples of Proterozoic gneiss in the wall zone transect range from 8.3 to 12.4 ‰ (Table 2). The location of each of the four samples was plotted in GIS and its distance from the Searchlight contact was determined (Table 2). No coherent pattern in δ18O values was discerned from this process.

Whole rock δ18O values for the five Ireteba granite samples range from 8.1 to 9.5 ‰, and whole rock δD values range from -87 to -98 ‰ (Table. 2). This correlates well with four previously analyzed Ireteba granite samples with whole rock δ18O values ranging from 8.2 to 8.8 ‰ (Kapp et al. 2002 and Townsend et al. 2000). The location of each of the five transect samples was plotted in GIS and its' distance from the Searchlight contact was determined. No pattern in Whole rock δ18O or δD values emerged.

Table 3. Sample distance to nearest contact and δ18O, δD values

Sample	IG_1	IG-2	IG-3	IG-4	IG-5	XG-10	XG-4	XG-5	XG-6
Distance from contact (km)	0.000	0.095	0.195	0.364	0.462	0.013	0.044	0.337	0.671
δ18O	8.9	8.1	9.5	8.9	8.5	8.3	12.4	10.3	10.7
δD	-94	-95	-87	-98	-94				
wt%H2O	0.3	0.4	0.4	0.3	0.4				

Compositional zoning in Monazite

Monazite has the nominal composition (LREE)PO_4 with La, Ce, and Nd generally comprising 75% of the total cation proportions (exclusive of P) of most metamorphic monazite (Spear and Pyle, 2002). In addition, most monazite also contains Th, U, Ca, Si, HREE's, Y, and Pb. Although HREE and Pb concentrations are usually insignificant the other elements can make up a substantial portion of monazite's cation budget (Spear and Pyle, 2002). While Pb is present in metamorphic monazite, it is believed to be entirely radiogenic (Spear and Pyle, 2002). The two primary substitutions responsible for Th and U incorporation into monazite are (from Spear and Pyle, 2002):

$$REE + P = Th \text{ or } U + Si \text{ (huttonite)} \quad (1)$$

$$2REE = Th \text{ or } U + Ca \text{ (brabantite)} \quad (2)$$

The validity of these two substitution mechanisms can be tested by plotting Th + U and Si + Ca atomic abundances. If these substitutions are responsible for the incorporation of Th, U, Ca and Si then the atomic abundances should plot along a line with a slope of one. Figure 10 shows that for samples of Proterozoic gneiss monazite Th + U / Ca + Si is close to one. Figure 10 shows that secondary zones in the Proterozoic gneiss monazite tend to be elevated in Si and Th content as compared to primary zones. Plots of Th + U vs. Ca and Th + U vs. Si indicated that the huttonite exchange is the primary path for Th and U to enter these monazite. Townsend (2000) showed the same trends in the Ireteba monazite. The Proterozoic gneiss monazite does not show a correlation between style or intensity of replacement zoning textures with distance from the contact with the Searchlight pluton. The Ireteba samples collected in this study do not show a correlation between style or intensity of replacement zoning with distance from the contact, but

samples collected by Townsend (2000) do show a spatial relationship. The Townsend samples were collected over a significantly larger portion of the pluton and are more representative of the pluton as a whole. In those samples the intensity of replacement is correlated with depth and proximity to Miocene plutons. The sample collected at greatest depth and closest to the Searchlight contact (in the same area as all the samples from this study) contained the most highly altered monazite.

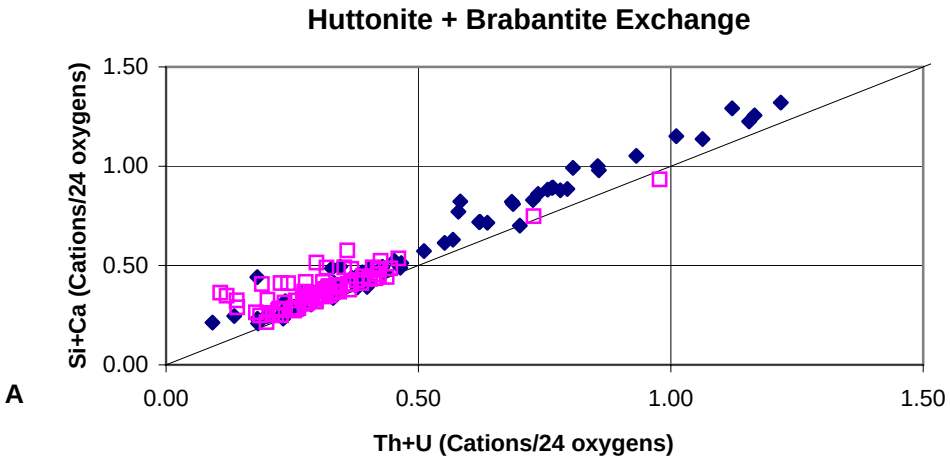

A

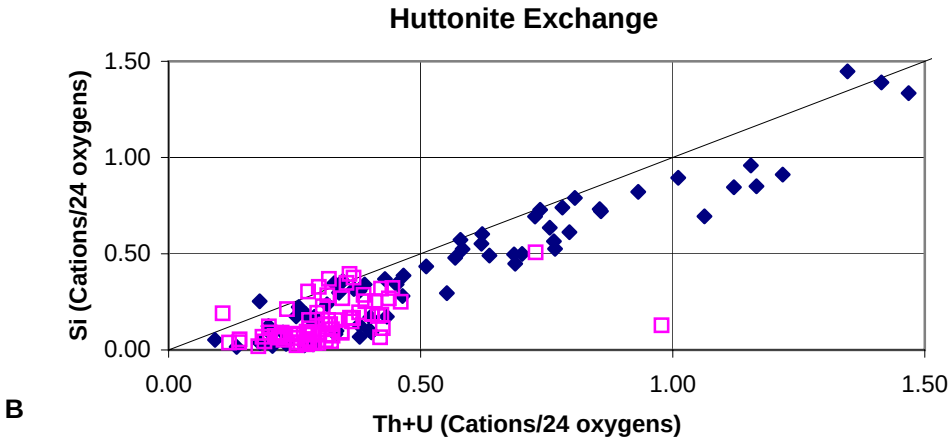

B

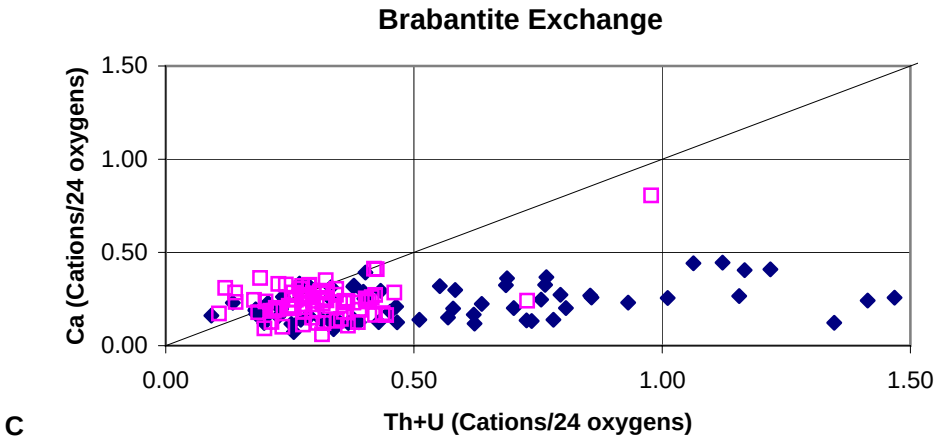

C

Figure 10. Concentrations of selected cations per 24 oxygen for Proterozoic samples. Primary zones are indicated by open squares and replacement zones are indicated by filled diamonds. (A) shows both huttonite and brabantite exchange, (B) shows the huttonite exchange as the primary exchange vector, (C) shows that brabantite accounts for very little of the Th and U substitution into monazite.

Monazite Geochronology

Both EMP chemical age dating and LA-ICP-MS isotope dating methods were used on the samples of Proterozoic gneiss. Because the EMP dates were not as precise as the LA-ICP-MS dates only the LA-ICP-MS age results will be presented here. Monazite was not found in all of the Proterozoic gneiss samples collected. Of the five samples of augen gneiss collected from the southern section of the roof zone only one, XG-2, yielded any monazite, and XG-2 only yielded a single monazite grain. However, LA-ICP-MS analyses of the XG-2 grain lacked sufficiently stable signals for dating so no age is reported.

The samples collected in the northern portion of the roof zone (XG-11), the wall zone (XG-4, XG-5, XG-6, and XG-10) and from the block in the lower Searchlight (XG-12) all yielded monazite. Monazites from these samples are mostly anhedral rounded grains 50 to 200 um in diameter. BSE imaging of monazite from all of these samples shows a wide variety of zoning within each sample. All of the wall zone samples and XG-11 contain monazites that are entirely patchy zoned as well as monazites that are a combination of patchy and concentric zoning. The mixed zoned monazite tended to have small interior concentrically zoned cores surrounded by large rims of patchy zoning. However, monazite that is entirely patchy zoned dominated in all samples (Fig. 11). Sample XG-12 from the country rock block contained entirely patchy zoned monazite. In some of the monazite grains zones display cross cutting relationships suggesting episodic growth or recrystallization of the monazite grains (Fig. 11).

208Pb/232Th ages of monazites from the wall zone samples (XG-5, XG-6, XG-10) range from 64.9 Ma to 1675 Ma with a primary peak in the probability density plot at

1635 Ma (Fig. 12). They also have a 206Pb/238U age range of 604 Ma to 1920 Ma and a peak in probability density at 1641 Ma. XG-6 has one 208Pb/232Th age of ~64 Ma (analysis of a highly complex patchy zone) which presumably corresponds to the intrusion of the Ireteba granite in the late Cretaceous. When plotted on concordia the wall zone monazite age analyses are mainly concordant and cluster around 1641 ± 16 Ma (Fig. 14). In addition, a probability density histogram of 207Pb/206Pb wall rock ages shows a unimodal age distribution with a peak at 1656 ± 3.5 Ma (Fig. 13). These ages are too young to represent the primary age of the Mojave super crustal sequence (>1.7 Ga). However, the ages may correspond to the 1.62 – 1.69 Ga intrusion of intermediate to felsic magma into the eastern Mojave terrain (Miller and Wooden, 1993). There does not seem to be a direct correlation between age and zone type in the wall rock samples.

Samples from the northern roof zone, XG-11, and the Proterozoic block in the lower Searchlight, XG-12, have 208Pb/232Th age ranges of 713 Ma to 1231 Ma and 430 Ma to 928 Ma respectively. These ages are highly discordant and do not represent real ages. A concordia plot of all wall zone samples, and samples XG-11 and XG-12 define a discordia line with an upper intercept at 1641±16 Ma and a lower intercept at 134±98 Ma (Fig. 14). Samples XG-11 and XG-12 have no concordant analyses.

The discordia defined by these analyses may represent a line of mixing between zones with ages at the lower intercept (which corresponds within error to the timing of intrusion of the Ireteba granite) and zones with ages of the upper intercept.

All five samples of Ireteba granite yielded monazite. The monazite grains are anhedral, rounded to angular, and range from ~50 um to ~200 um in diameter. BSE images show both patchy zoned and concentrically zoned monazite as well as monazite that have

combinations of concentric and patchy zoning. Monazite with patchy zoning and no concentric zoning appears to dominate in the collected samples. LA-ICP-MS analysis of all Ireteba samples yields a bimodal age distribution in 208Pb/232Th (Fig. 15). 208Pb/232Th ages have a range of 15.1 Ma to 61.1 Ma and major peaks at ~17.4 Ma and 53.8±0.6 Ma. The lower peak (17.4 Ma) falls with in the Searchlight age range (15.7 to 17.7 Ma) while the older peak (53.8 Ma) is close but does not exactly relate to the primary (66 Ma) age of the Ireteba granite. This suggests that analyses of primary zones often included portions of young age zones. Concordia plots of the analysis were less conclusive. The data still displayed a distinct bimodality but few of the data points are concordant, and the discordant analyses do not define a meaningful line of discordia.

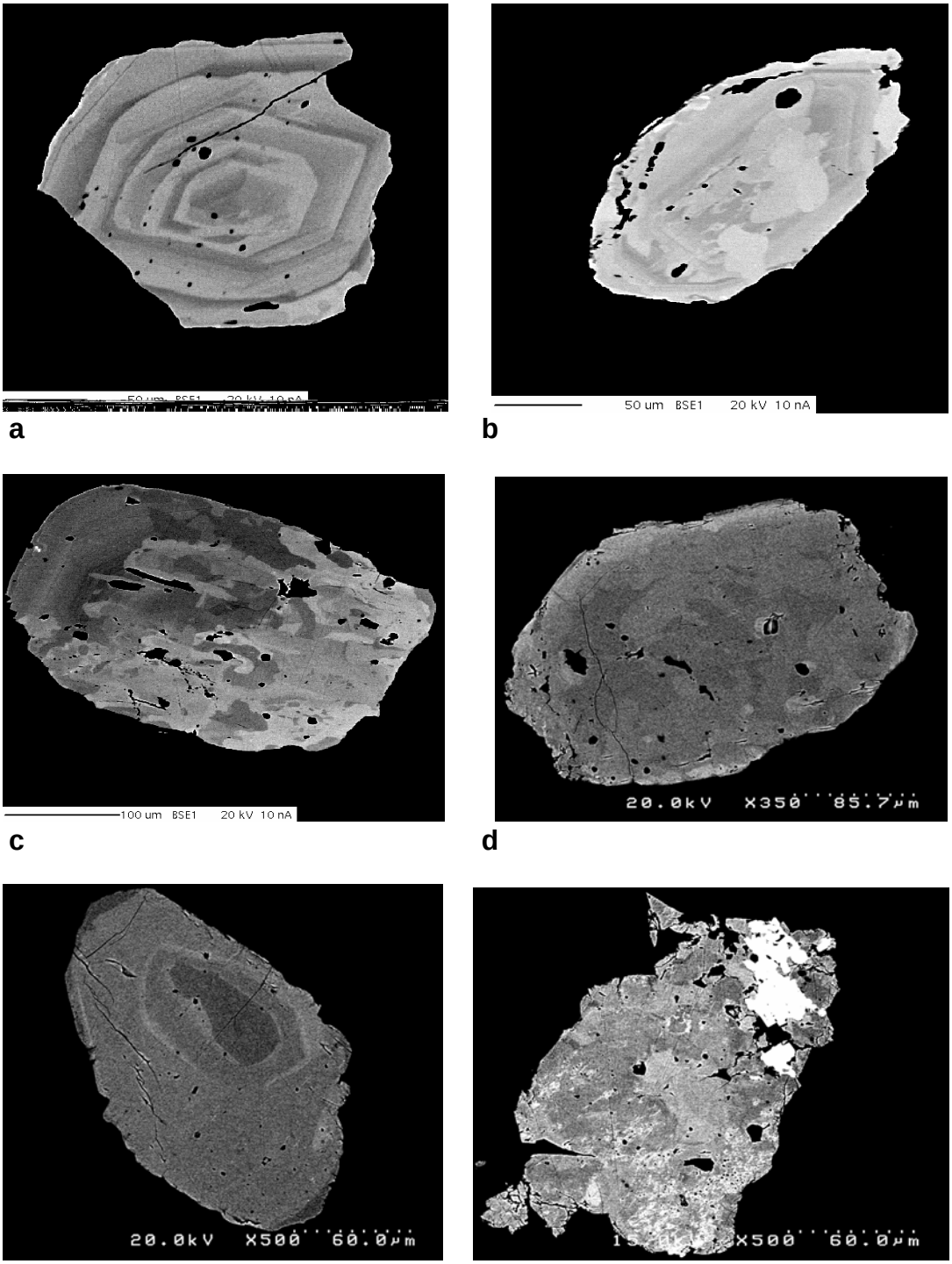

Figure 11. BSE images of monazite displaying different types of zoning. a, IG-3mon6 concentric magmatic zoning; b, IG-2mon15 patchy zoning overprinting concentric zoning; c, IG-5mon3 patchy and concentric zoning; d, XG-4mon3 patchy zoning; e, XG-4mon32 core with overgrowth; f, XG-6mon23 complex patchy zoning. Images a,b,c are all from University of Tennessee's Cameca SX-50 electron microprobe. Images d,e,f were taken at the University of Vanderbilt on the Hitachi S-4200 Scanning Electron Microscope.

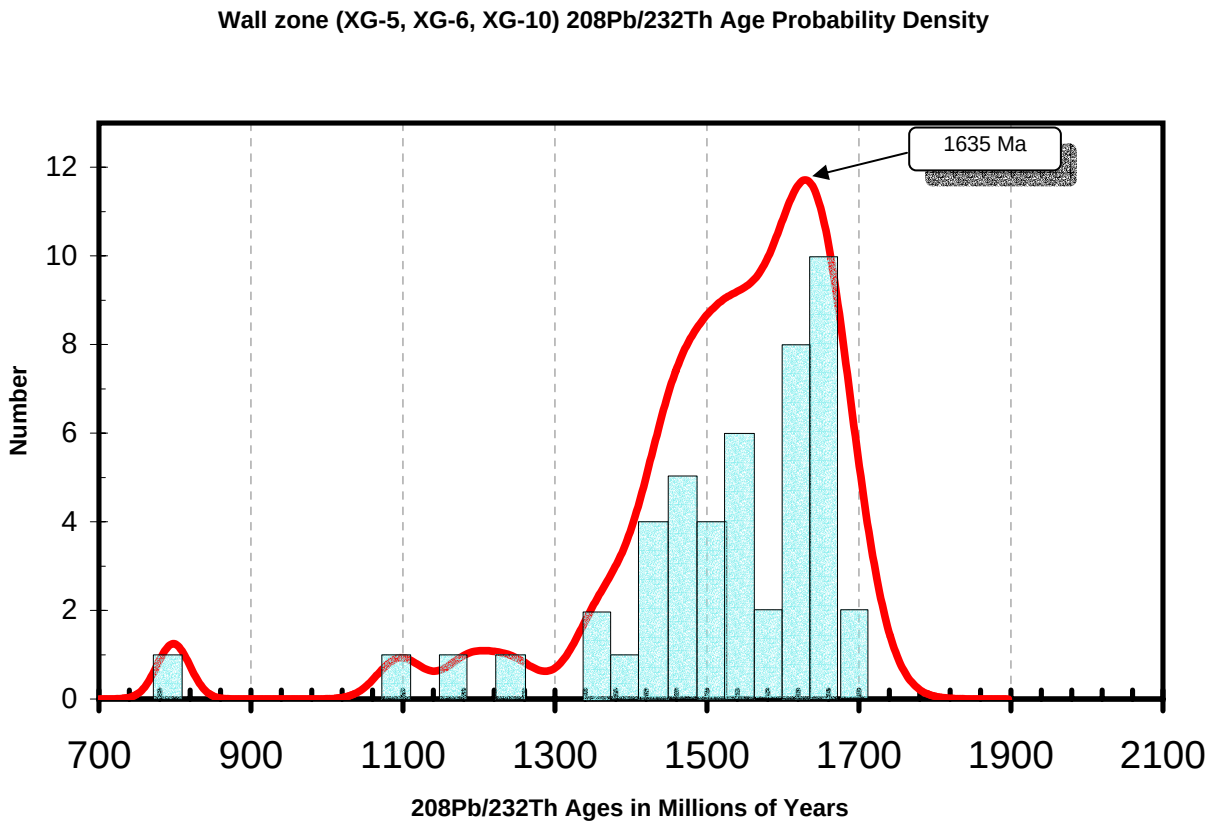

Figure 12. Cumulative probability histogram of Wall zone Proterozoic gneiss samples XG-5, XG-6 and XG-10. Sample XG-4 is not included because the data was deleted in reprocessing. The spread in the data suggest lead loss or mixed zone analyses. The 207/206 age data from these analysis seems to be more accurate.

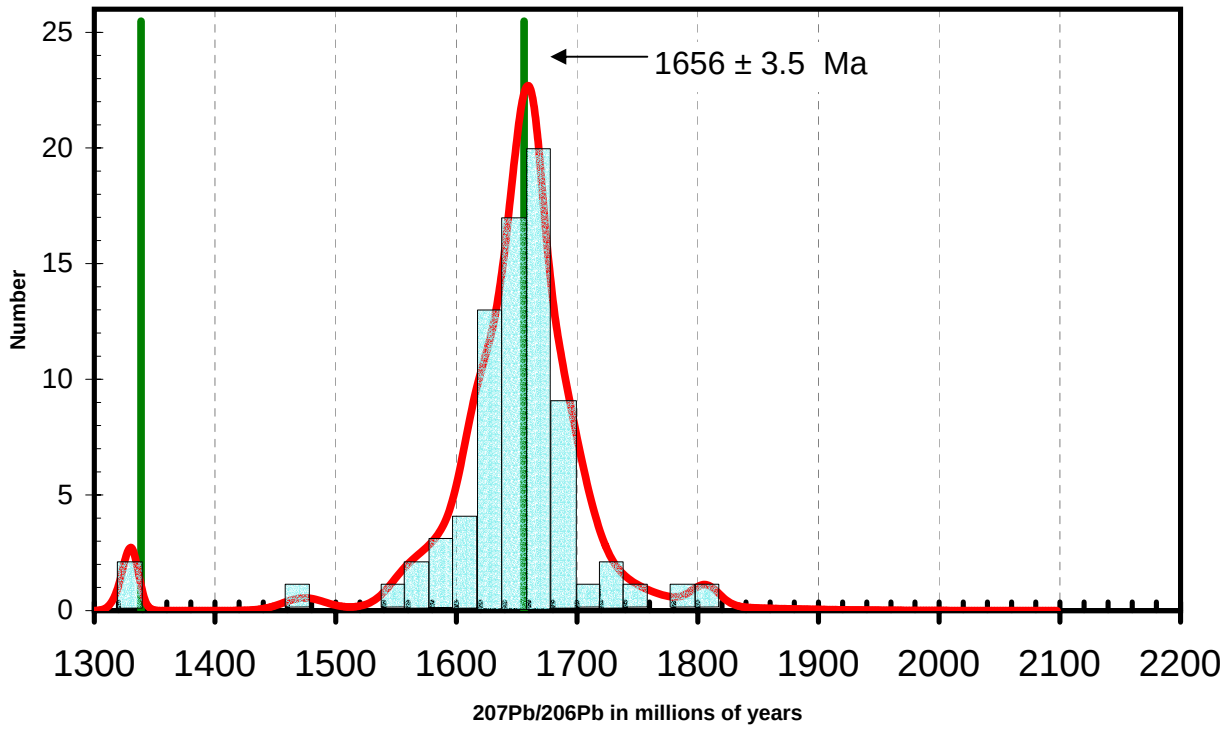

Figure 13. Cumulative probability histogram of wall zone Proterozoic samples and XG-11 and XG-12 clearly demonstrating a unimodal age population for the monazite in these rocks. The peak age is with in error of the upper intercept of the concordia diagram in fig. 13. The two small peaks out side the main population likely correspond to the discordant analyses in XG-11 and XG-12.

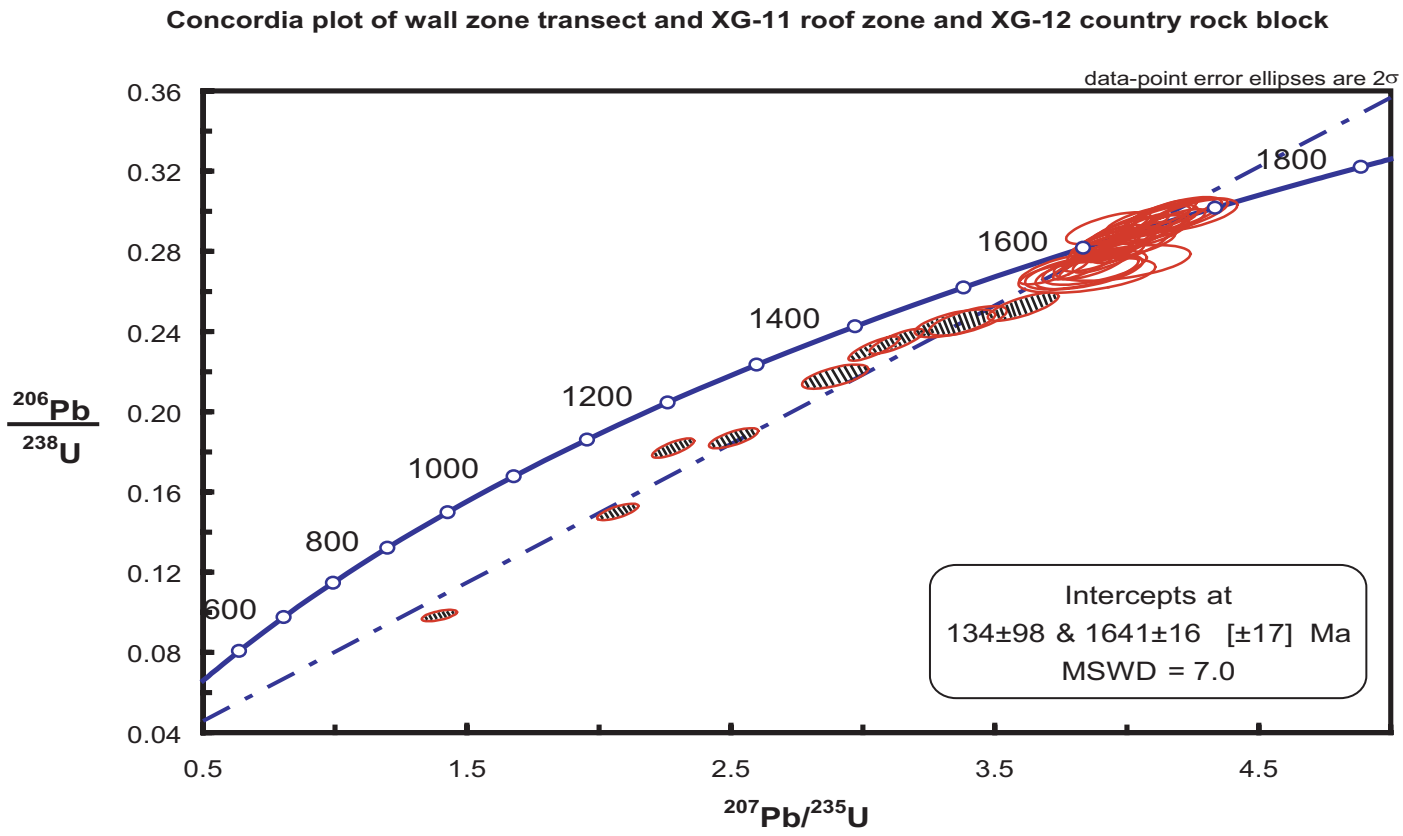

Figure 14. Concordia diagram for all Proterozoic wall zone samples and XG-11 and XG-12. Ellipses with hash marks represent analyses from XG-11 and XG-12

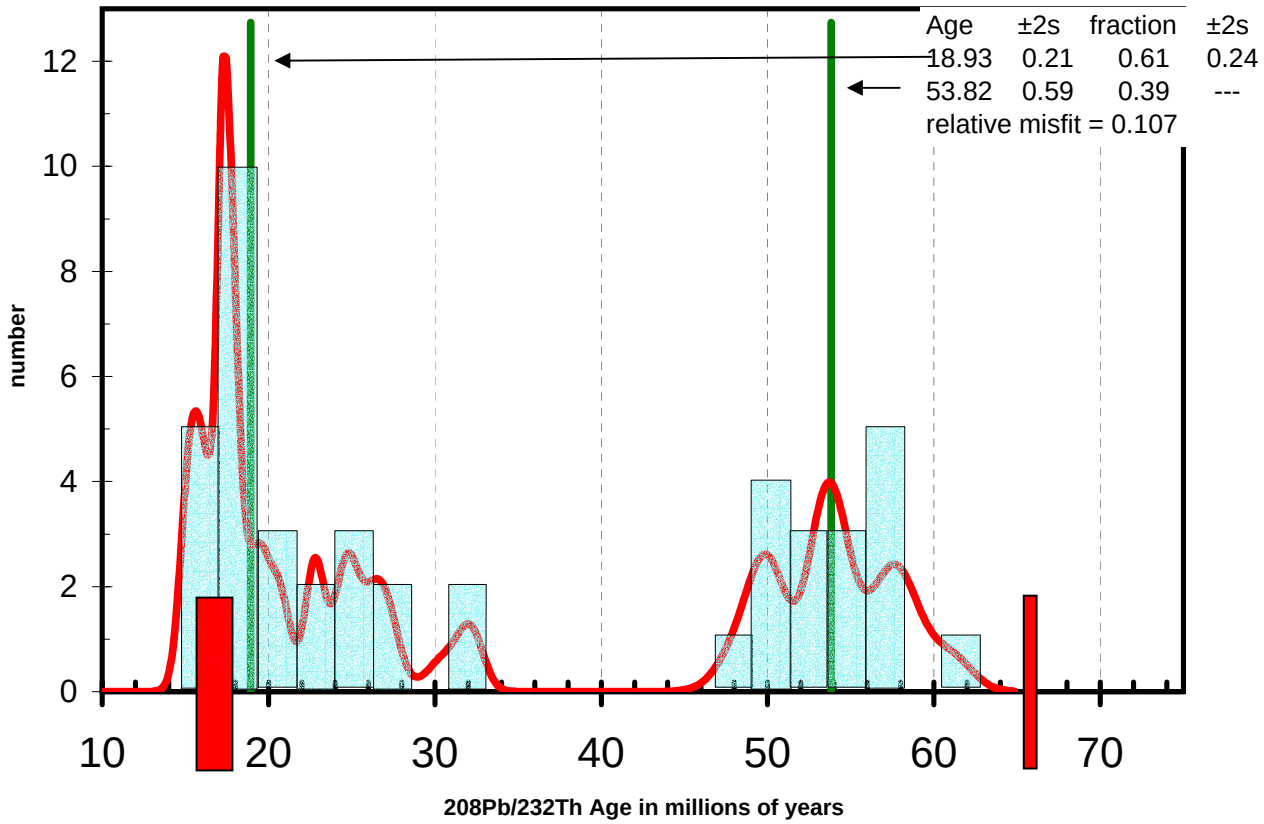

Figure 15. Cumulative probability histogram of Ireteba granite monazite with bimodal age distribution. Green lines indicate the age calculated by Isoplot unmixing program. The short red bars on the x-axis represent the actual ages of the Searchlight pluton (15.7 to 17.7 Ma and the Ireteba pluton 66 Ma. The plotted ages fall between the two real ages because analyses overlapped age zones. The major peak next to the lower green bar is at 17.4 Ma which falls within the upper end of the Searchlight age range.

Table 4. LA-ICP-MS Age Data For Ireteba Granite Monazite Samples

sample	Grain #	spot #	$^{208}Pb/^{232}Th$ Age (ma)	1σ error	$^{206}Pb/^{238}U$ Age (Ma)	1 σ error	$^{207}Pb/^{235}U$ Age (Ma)	1 σ error
IG-1	1	10	17.3	0.48	23.9	0.52	120.2	3.87
IG-1	1	11	17.9	0.52	24	0.62	64	4.61
IG-1	1	12	18.9	0.74	59.5	2.36	525.3	23.66
IG-1	2	13	17.2	0.27	-	-	-	-
IG-2	21	6	50.3	1.47	54	2.22	144.9	18.01
IG-2	19	7	48.6	1.4	41.1	1.13	203.3	8.39
IG-2	15	8	30.7	1.11	17.5	0.62	24.9	9.59
IG-2	25	9	22.7	0.74	23.5	1.32	60.5	9.71
IG-2	18	10	58	1.66	91.1	3.97	480.5	29.83
IG-2	26	11	17.7	0.58	35.3	0.65	222.8	5.48
IG-3	7	43	26.2	0.76	24.3	0.83	42.1	8.96
IG-3	7	44	53.6	1	58.7	1.39	80.6	20.09
IG-3	7	45	50	0.99	48.7	2.03	148.4	13.78
IG-3	6	50	57.7	1.21	85	3.57	291.1	21.56
IG-3	6	51	50.1	1.17	58.8	2.27	238.8	15.99
IG-3	6	52	61.1	1.26	156.7	4.66	959.9	33.75
IG-3	5	53	53.5	1.05	57.7	1.09	68.9	27.03
IG-3	5	54	54.5	1.06	69.9	3.21	222.2	18.68
IG-3	5	55	57.7	1.33	62.1	2.22	138.7	19.16
IG-3	27	60	54.2	1.09	53.5	2.35	86.4	33.45
IG-3	27	61	53.2	1.05	46.1	1.87	129.9	14.12
IG-3	20	62	53.3	1.11	64.3	2.84	141.3	21.04
IG-3	20	63	26	1.18	25.2	1.12	95.6	7.91
IG-4	1	20	24.8	0.61	43.2	1.09	55.7	21.26
IG-4	1	21	27.2	0.73	22.9	0.57	38.2	5.92
IG-4	1	22	19.9	0.73	31.9	0.76	47.6	9.77
IG-4	1	23	24.4	0.74	24	1.23	64	8.81
IG-4	7	24	17.5	0.45	21.3	0.94	80.5	6.12
IG-4	7	25	20.8	0.56	27.2	1.59	80.8	12.93
IG-4	7	30	16.1	0.47	32.2	1	279	10.14
IG-4	23	31	15.1	0.54	-	-	-	-
IG-4	23	32	22.8	0.51	39	1.44	338.3	14.57
IG-4	25	33	17.6	0.55	20.5	0.85	56.8	5.91
IG-4	25	34	32.2	0.74	25.3	0.78	35.4	11.90
IG-4	10	35	17	0.65	21.6	1.27	97	8.89
IG-4	10	40	17.7	0.49	25.6	0.98	66.9	6.83
IG-4	10	41	17.3	0.54	24.1	0.88	122.2	6.64
IG-4	21	42	19.4	0.65	23.5	0.92	78.2	6.00
IG-5	26	14	49.1	1.56	67.8	2.58	206.1	18.47
IG-5	10	15	15.3	0.49	19.6	1.25	85.3	9.96
IG-5	1	16	15.4	0.68	17.4	0.24	21.2	6.33
IG-5	3	17	57.8	1.69	60.5	1.94	136.3	18.80
IG-5	33	18	56.6	1.64	73.7	3.65	229.2	26.61
IG-5	32	19	15.9	0.55	25.5	1.76	112.9	12.53

Table 5. LA-ICP-MS Age Data for Proterozic Gneiss Monazite Samples

sample	Grain #	spot #	$^{208}Pb/^{232}Th$ Age (ma)	1σ error	$^{207}Pb/^{206}Pb$ Age (Ma)	1 σ error	$^{206}Pb/^{238}U$ Age (Ma)	1 σ error	$^{207}Pb/^{235}U$ Age (Ma)	1 σ error
XG-4	1	10	-	-	1665.8	6.9	1802.3	3.01	1740.3	7.77
XG-4	1	11	-	-	1654.6	9.38	2482.1	5	2057.4	12.38
XG-4	6	12	-	-	1668.1	8.95	-	-	-	-
XG-4	6	13	-	-	1652.9	10.08	1637	3.47	1644.3	10.62
XG-4	10	14	-	-	1640.1	10.94	1854.4	4.16	1756	12.36
XG-4	10	15	-	-	1705.4	13.01	1520.3	3.98	1599.8	12.90
XG-4	11	25	-	-	1661.6	7.09	3366.3	5.6	2402.2	11.00
XG-4	11	26	-	-	1653	7.88	-	-	-	-
XG-4	2	27	-	-	1687.2	12.66	1582.2	4.04	1628.1	12.90
XG-4	2	28	-	-	1664.4	9.08	1696.7	3.37	1682.7	9.77
XG-4	19	29	-	-	1655.1	7.89	1764	3.2	1715.1	8.75
XG-4	19	30	-	-	1645.3	8.67	1775.9	3.41	1717.1	9.63
XG-4	3	40	-	-	1620.6	12.37	1612.9	3.98	1616.6	12.97
XG-4	3	41	-	-	1612.2	10.7	1639.7	3.62	1628	11.39
XG-4	3	42	-	-	1682	15.91	1551	4.79	1607.7	16.00
XG-4	5	43	-	-	1643.2	11.21	1855.1	4.28	1757.7	12.66
XG-4	5	44	-	-	1806.5	11.29	2337	5.69	2066.8	13.86
XG-4	9	45	-	-	1621.9	14.73	1619.3	4.59	1620.7	15.42
XG-5	1	58	-	-	1796.1	78.75	984.7	14.7	1271.8	58.91
XG-5	2	59	-	-	1629.5	15.52	1683.8	5.03	1659.9	16.57
XG-5	2	60	-	-	1653.4	27.93	1939.4	9.99	1805.2	31.88
XG-5	10	61	-	-	1696.1	43.82	1533.1	12.35	1603.1	43.38
XG-5	11	9	1647	43.72	1677.2	15.04	1658.6	15.59	1666.4	21.65
XG-5	11	10	1638	43.48	1667.2	22.3	1748.7	17.55	1711.5	28.62
XG-5	12	11	1438.1	38.45	1651	19.51	1603.3	15.75	1623.5	24.95
XG-5	12	12	1449.4	38.81	1679.7	17.58	1681.8	16.18	1680.4	23.89
XG-5	3	13	1244.6	33.36	1331.5	5.68	-	-	-	-
XG-5	3	14	1350.2	36.12	1326.5	7.67	-	-	-	-
XG-5	4	24	1540.2	41.01	1697.8	19.13	1704.9	16.79	1701	25.45
XG-5	5	25	1663.8	44.21	1661.1	12.28	1685.8	15.67	1674.1	19.88
XG-5	5	26	1511.3	40.34	1650.1	51.46	2165.7	30.73	1912.7	65.53
XG-5	19	27	1644.9	43.68	1665.9	13.37	1647.7	15.5	1655	20.46
XG-5	19	28	1621	43.05	1638.1	16.79	1600.8	15.53	1616.2	22.81
XG-5	6	29	1611.8	42.83	1686.5	26.01	1742.2	18.48	1716.3	32.13
XG-5	6	39	1393	37.19	1657.8	14.33	1765.9	16.76	1716	22.03
XG-6	10	40	1623	43.22	1661.3	15.53	1626.7	15.75	1641	22.09
XG-6	10	41	1638.1	43.52	1689.5	30.04	1549.9	17.54	1609.1	33.91
XG-6	23	42	64.9	2.08	3311.5	65.85	493.1	13.56	1399.1	47.48
XG-6	8	43	1640.4	43.57	1647	31.1	1905	21.31	1783.8	39.15
XG-6	23	44	1669	44.27	1692.8	18.46	1450.8	14.74	1551.1	23.12
XG-6	19	54	798	21.66	1637.3	19.12	1820.8	18.12	1735.8	26.63
XG-6	6	55	1675.9	44.51	1637.3	19.12	1820.8	18.12	1735.8	26.63
XG-6	6	56	1474.5	39.29	1694.2	31.33	1539.3	17.85	1604.7	35.03
XG-6	6	57	1184.5	31.79	1679.8	33.86	1540	18.36	1598.9	37.44
XG-6	4	58	1470.4	39.25	1652	27.08	1637.7	17.93	1642.9	32.39
XG-6	4	59	1450.1	38.69	1643.2	15.78	1664.9	16.33	1654.2	22.71
XG-6	7	69	1550.5	41.31	1620.4	13.77	1753.2	16.97	1692.3	21.80
XG-6	1	70	1573.2	41.9	1683.7	16.92	1601.7	16.09	1636.3	23.25
XG-6	9	71	1471.3	39.21	1657.2	23.54	1682.6	17.83	1670.1	29.60
XG-6	9	72	1430.6	38.24	1660.6	17.58	1579.6	15.99	1613.5	23.63

Table 5. Continued

sample	Grain #	spot #	$^{208}Pb/^{232}Th$ Age (ma)	1σ error	$^{207}Pb/^{206}Pb$ Age (Ma)	1 σ error	$^{206}Pb/^{238}U$ Age (Ma)	1 σ error	$^{207}Pb/^{235}U$ Age (Ma)	1 σ error
XG-10	6	84	1679.4	44.62	1658.7	16.03	1815.1	18.04	1742.3	24.15
XG-10	6	85	1601.1	42.66	1637.6	45.59	1917.5	26.03	1785.6	55.31
XG-10	3	86	1622.7	43.11	1671.8	26.72	1756.3	19.39	1716.8	33.35
XG-10	3	87	1613.2	42.9	1676.3	26.78	1762.4	19.5	1722.1	33.47
XG-10	8	88	1096.3	29.53	1635.6	23.81	1414.2	15.46	1504	27.38
XG-10	27	89	1668	44.37	1679.7	15.31	1576.8	15.92	1620.1	22.04
XG-10	31	90	1617.6	42.97	1580.6	44.02	1910.6	22.65	1757	53.18
XG-10	31	91	1644.3	43.66	1668.4	40.64	1920.9	22.28	1802	48.62
XG-10	30	92	1666.8	44.28	1612.9	17.06	1877.5	18.04	1755	25.08
XG-10	14	93	1444.2	38.68	1637	24.45	1666.3	17.03	1653.2	29.92
XG-10	15	94	1523.8	40.57	1637.9	21.21	1793.6	17.82	1722.8	28.12
XG-10	19	95	1631.7	43.37	1608.2	27.56	1897	19.6	1763.4	35.29
XG-10	11	9	1505	38.55	1627.8	22.66	1610.5	15.84	1623.7	27.68
XG-10	11	10	1528.9	39.15	1571.6	23.28	1649.3	16.2	1620.2	28.80
XG-10	29	11	1556.7	39.84	1665.1	27.97	1681.3	17.22	1678	33.01
XG-10	2	12	1555.3	39.79	1633.7	29.97	1758.9	18.23	1705.5	35.94
XG-10	1	13	1516.6	38.84	1654.4	28.93	1612.6	16.71	1632.9	33.19
XG-10	26	14	1360.6	35	1661	12.08	1600.9	14.91	1628.3	19.24
XG-10	26	15	1485.6	38.08	1619.5	17.71	1544.4	14.85	1576.8	22.96
XG-10	24	16	1530.2	39.19	1721.2	41.62	1562.2	18.43	1630.6	43.87
XG-10	24	23	1572.8	40.26	1662.1	15.8	1740.6	16.5	1698.4	22.80
XG-11	1	24	1231.9	31.78	1632.5	26.71	1407.9	14.62	1492.6	28.92
XG-11	2	25	1215	31.39	1577.6	25.16	1268.6	13.09	1380.5	26.22
XG-11	3	26	874	22.75	1597.8	19.51	1104	11.14	1275	20.20
XG-11	4	27	1219.6	31.46	1557.7	13.78	1342.4	12.96	1418.1	18.57
XG-11	4	28	1199.6	30.99	1582.9	14.8	1361.4	13.21	1439.6	19.40
XG-11	4	29	786	20.6	1473.9	17.68	1077	10.77	1206.3	18.84
XG-11	1	30	713.3	18.67	1759	38.16	774.9	9.28	1068.7	26.48
XG-12	1	40	430.9	11.37	1726.5	28.19	604.8	6.78	886.9	17.57
XG-12	1	41	928.3	24.14	1678.6	19.59	901.2	9.39	1139.3	17.82
XG-7	1	73	16	0.92	2622.1	327.82	28.7	3.04	104.6	17.14
XG-7	1	74	16.7	0.86	3977.6	275	24.3	3.32	200.1	30.64

CHAPTER IV

DISCUSSION

The two primary ways for fluids to infiltrate the country rock are porous flow and dike or vein transport. Here we are attempting to evaluate the broader effects of porous flow rather than localized effects due to dike and vein flow. Quartz veins (as large as 1m thick) are prominent along the contact of the middle Searchlight unit and the Proterozoic wall zone rocks. Smaller and less abundant quartz veins can be found along the Searchlight Ireteba contact. During sample collection these veins were avoided to minimize the possibility of localized fluid effects on monazite. However, sample XG-10 was collected adjacent to the contact and proximity to quartz veins was unavoidable.

Monazite from country rock gneiss and granite surrounding the Searchlight pluton shows evidence of having been partially or in some cases wholly recrystallized. BSE imaging shows chemical zonation within individual monazite from all samples collected along the Searchlight contact. Monazite from the Searchlight country rock displays two main types of zoning. Concentric zoning is interpreted to be primary magmatic zoning. Patchy zoning is interpreted to result from the recrystallization of monazite, and it usually overprints the primary concentric zoning. Recrystallization could be caused by interaction with hydrothermal fluids or it could result from a combination of heat and strain. Many of the monazites in this study consist of a combination of concentric and patchy zoning. All types of zones are characterized by sharp contacts at the micron scale suggesting that bulk chemical diffusion is not the cause of zonation.

Monazite from the Proterozoic gneiss wall zone (samples XG-4, XG-5, XG-6, XG-10) display both types of zoning but are primarily patchy or combination zoned. However, all the monazites from these samples are nearly concordant defining an upper intercept for discordia at 1641±16 Ma, and have a unimodal 207Pb/206Pb age distribution with a mean age of 1656±3.5 Ma. The lack of Miocene ages in the monazite implies that the intrusion of the Searchlight pluton ~17 Ma to 15 Ma was not responsible for the chemical zonation of the monazite observed in BSE images. Whole rock oxygen isotope analysis of these samples shows some variability in δ18O values in the wall zone rocks (8.30‰ to 12.4‰) though it follows no specific spatial pattern related to the Searchlight contact and is significantly different from previously obtained δ18O values for middle and lower Searchlight rocks (δ18O ~7.0‰) (Bachl et al., 2001). Replacement zoning in monazite from these samples is likely the result of an older geologic event. The Mojave super crustal terrain has a ~ 2 billion year old history over which several major regional geologic events occurred. Specifically, the terrain was intruded by abundant felsic magmas between 1.62 Ga and 1.69 Ga (Wooden and Miller, 1990). The augen orthogneiss located in the southern roof zone may be part of this batholithic scale magmatic event. Presumably the ~1650 Ma age of the Mojave super crustal wall zone rocks corresponds to this intrusion event and fluids involved with it.

Samples XG-11 and XG-12 are from the northern roof zone and a country rock block located in the upper portion of the lower Searchlight unit respectively. The monazite in XG-11 is entirely combination zoned while monazite in XG-12 is entirely patchy zoned. In sample XG-11 and XG-12 Th-Pb and U-Pb ages cover wide ranges of 713 Ma to 1231 Ma and 430 Ma to 928 Ma respectively. None of the analyses from the

two samples are concordant. However, when plotted with Proterozoic wall zone samples (XG-4, XG-5, XG-6, and XG-10), XG-11 and XG-12 define a distinct line of discordia with an upper intercept at 1641± Ma and a lower intercept at 134±98 Ma (fig. 15). The lower intercept is poorly defined because of a lack of ages younger than 430 Ma. However, this line could be interpreted as a mixing line between zones of older Proterozoic ages and younger possible Miocene or Cretaceous ages related to the Searchlight or Ireteba plutons. In both samples XG-11 and XG-12 the zoning in the monazite was intricate, making it difficult to avoid sampling multiple zones during ablation and resulting in the series of mixed ages. The location of these two samples likely contributed to their recording possible interaction with Searchlight hydrothermal fluids. Sample XG-11, located in the northern roof zone directly above the upper Searchlight unit and below Miocene volcanics, may have been in position to interact with fluid that was released directly from the upper unit. Sample XG-12, located on the margin of a country rock block in the upper portion of the lower Searchlight unit, could have experienced considerable interaction with magmatic fluids. In addition, it is likely that the block experienced considerable heating during its residence in the middle of an active magma chamber.

Monazite from Ireteba granite samples (IG-1, IG-2, IG-3, IG-4, and IG-5) more clearly document alteration related to the intrusion of the Searchlight pluton. The Th-Pb isotope system in all five samples displays a bimodal age distribution with a primary peak at ~17 Ma and a peak at ~53 Ma. However, there is little evidence to suggest the alteration resulted from hydrothermal fluids. Petrography indicates very fresh rock with little or no alteration minerals. In addition, a strong ductile deformational fabric pervades

these rocks. If these rocks were behaving ductilely it is likely that any pore spaces would be sealed disallowing porous flow through the rocks. Whole rock oxygen isotope analysis show minimal variation in δ18O values (8.1‰ to 9.5‰), and no systematic changes with distance from the Searchlight contact. In addition, hydrogen isotope analysis of the Ireteba samples shows variation (-87‰ to -98‰) but no pattern related to distance from the Searchlight contact. Had hydrothermal fluids been released into these rocks from the Searchlight pluton it is likely that these isotope systems would have recorded its movement by altering the Ireteba isotope signature to look more like that of the Searchlight (δ18O of 7.0‰). If the fluid rock ratio in this zone was small it is possible that the Ireteba granite could have buffered the δ18O of the infiltrating fluids causing the signature of the Searchlight to be masked. Hydrogen isotopes are less susceptible to this effect because the country rocks contain much less exchangeable hydrogen than oxygen. Hydrogen isotopes should therefore be even more sensitive to alteration from infiltrating fluids. Yet, even this system does not show a distinct pattern related to the Searchlight pluton, further supporting the theory that little or no fluid was released by the Searchlight pluton into the northern margin wall rocks. However, the fact remains that monazite from the Ireteba granite records alteration at the time of the Searchlight intrusion.

In previous studies of the Ireteba granite Townsend (2000) and Loflin (2002) reported monazite alteration increasing with paleodepth and proximity to the Searchlight contact. The most altered monazite came from approximately the same depth and area of deformation as the samples in this study. Current evidence may suggest that alteration of monazite in the Ireteba is related to heating and stress resulting from the emplacement of

the Searchlight Pluton. This interpretation may also suggest why no Miocene replacement of monazite occurred in the Proterozoic wall zone. The Proterozoic wall zone would have been located above the Ireteba granite and appears to have behaved rigidly as apposed to the more ductile behavior along the Ireteba-Searchlight contact.

Samples of Proterozoic augen orthogneiss from the southern roof zone (XG-1, XG3 and XG-13) did not contain monazite and sample XG-2 contained a single grain. Sample XG-2 is a peraluminous augen orthogneiss with an appropriate composition for the inclusion of monazite. The fact that only one monazite was found in XG-2 and that no monazite was found in similar samples (XG-1, XG-3 and XG-13) suggests either an initial lack of monazite (it is possible that these rocks were more metaluminous in composition) or that initial monazite was reacted out of the rocks. Mineralogical and petrographic evidence suggest large quantities of fluids moved through these rocks. These rocks contain large amounts of epidote and opaques and even some calcite, all minerals associated with hydrothermal alteration. In addition these rocks stratigraphically lie between the Upper Searchlight unit and highly altered Miocene volcanics. The overlying Miocene volcanics contain the vast majority of the hydrothermal ore deposits in the area. It is likely that much of the alteration in the augen orthogneiss is related to fluids released from the upper Searchlight unit. Evidence indicates that magmatic fluids from the Searchlight were highly oxidized. They may have reacted with monazite, converting Ce^{3+} into Ce^{4+} creating the potential for chemical reactions with surrounding mineral phases that would consume the monazite. Ce^{3+} is the primary LREE constituent of monazite, $(LREE)PO_4$, so any reactions that consume it are likely to adversely affect the stability of monazite.

Possibly the upper Searchlight unit was responsible for most of the fluid release from the pluton. This fluid, once released, circulated through the Miocene volcanics and some portion of the shallow northern roof zone Proterozoic gneiss (i.e. XG-11) but was unable to penetrate deeper, thus preventing fluid alteration of the monazite at the level of the transect collected in the Proterozoic wall zone.

CHAPTER V

CONCLUSIONS

Three distinct generations of monazite growth have been identified in the Searchlight country rock; ~1650 Ma, ~66 Ma, and ~17 Ma. The younger generations were identified in the past by Townsend (2000). However, this study shows that the 66 Ma (age of Ireteba pluton emplacement) and 17 Ma (age of Searchlight pluton emplacement) country rock ages are confined to the Ireteba pluton. The oldest generation, 1650 Ma, was identified in the northern wall zone biotite - rich paragneisses and garnet - rich leucogranite of the Mojave supercrustal sequence. The monazite in the wall zone Proterozoic rocks lack any Miocene ages and only one analysis on one grain gave a Cretaceous age suggesting they were unaffected by the emplacement of the Searchlight pluton and that the Ireteba had a very little effect. Monazite from both the Proterozoic rocks and Ireteba granite has pervasive patchy zoning. However, evidence for fluid alteration of monazite in the Ireteba granite is cryptic at best. This suggests that using patchy zoning as a diagnostic feature of hydrothermal alteration may be questionable. Though no datable monazite was recovered from the augen orthogneiss of the southern roof zone, hand sample and petrographic evidence suggest these were highly fluid altered rocks. This combined with the lack of monazite alteration in the Proterozoic wall rocks, the cryptic evidence for fluid alteration in Ireteba monazite, and the location of the major ore bodies in the roof zone points to a focused release of fluid through the roof of the Searchlight pluton.

Appendix A

Monazite Elemental Concentrations

In ppm measured with

Cameca SX-100 at RPI

Table 1. Monazite Element concentrations in Parts per million as Measured on Cameca SX-100

spot#	sample	grain	Si	P	Ca	Y	La	Ce	Pr	Nd	Sm	Gd	Th	U	Tb	Dy	Er	Pb avg
9	xg9	4	13230.52	111659.07	12024.29	901.91	71005.04	192940.07	25308.30	110056.39	18951.05	7067.80	113184.71	2149.78	858.32	149.22	-12.33	10814.33
10	xg9	4	7243.00	121028.99	10277.73	936.23	87989.78	220050.43	27456.48	111288.57	19325.84	10097.02	67998.73	2171.59	345.41	605.12	269.88	7223.99
11	xg9	4	772.09	130960.63	9185.14	19720.92	114200.17	234236.43	25684.23	90729.91	16450.55	13723.76	25533.51	10316.53	1515.47	6659.71	1704.01	5315.20
12	xg9	5	735.02	131153.04	9270.27	22945.27	108663.32	230276.46	24985.23	96038.34	17595.18	15051.01	25071.69	11341.07	1945.24	7880.89	2268.78	5352.40
13	xg9	5	630.75	130288.34	8594.77	9406.55	110915.92	240261.13	26335.72	102506.85	19989.06	16959.36	26631.90	5497.55	2136.78	5414.41	649.50	3947.23
14	xg9	5	1616.23	127176.68	11708.39	3630.94	102508.03	232816.06	26918.49	104129.38	19953.78	14711.78	44157.18	4258.51	1197.53	2091.41	282.32	5312.05
15	xg9	5	12931.68	111923.53	10082.83	838.91	74429.70	201261.46	26076.02	113776.24	19732.37	7340.78	98556.64	2018.66	647.38	264.81	291.82	7865.83
16	xg9	2	769.82	131653.39	4858.19	18260.42	122514.35	252461.81	26524.35	97968.83	17808.75	15125.84	20440.91	324.27	1847.83	6976.39	1454.44	67.58
17	xg9	2	8108.81	121493.16	12082.17	1056.72	75191.37	211680.11	27784.55	119450.51	20674.47	6735.63	79161.87	1850.19	432.61	307.09	69.61	7675.74
18	xg9	2	16250.20	106943.86	10841.85	374.59	69023.02	190397.74	24678.36	107430.34	17444.73	7813.10	117235.40	3529.61	-131.23	379.66	175.90	10845.02
19	xg9	2	6095.97	123683.60	11180.55	1046.99	86639.06	223692.70	27432.86	116304.22	20299.82	8815.68	65851.80	1888.58	296.32	224.93	-5.74	6553.04
20	xg9	2	580.25	131248.97	9091.74	20439.21	115957.70	234951.22	25004.79	93824.84	15677.24	13965.92	24064.56	10380.08	1719.83	6911.13	1949.51	4904.24
21	xg9	2	1587.63	130134.90	8330.34	13073.92	108075.83	238155.85	26811.52	102552.63	18667.19	13658.62	29128.83	7409.26	1279.67	5324.44	920.38	4624.63
22	xg9	2	27976.19	100216.62	1708.26	79104.79	65209.68	137963.75	14710.26	60292.42	9251.93	18060.14	91930.53	35232.88	3070.39	19768.52	6858.57	651.72
23	xg9	3	10170.33	118927.41	10153.74	360.89	81702.01	211218.21	27136.03	110636.21	19516.17	7678.82	82538.37	2171.33	447.15	452.79	18.28	8091.62
24	xg9	3	10287.09	118990.78	10144.71	452.16	81462.21	213283.70	27085.09	110333.31	19391.21	8958.89	82089.35	2116.68	651.95	312.27	146.56	8193.31
25	xg9	3	626.98	133580.80	9117.39	22889.22	110848.56	232804.96	24978.62	93427.12	16503.83	14642.23	24193.19	10284.08	1466.27	7513.40	2102.36	4871.08
26	xg9	3	736.64	132069.38	9294.57	22101.12	109855.70	230910.91	25005.30	95152.10	16845.10	14628.55	24829.47	10661.07	1779.43	7314.06	1877.33	5077.41
27	xg9	3	769.20	131645.45	8087.94	7713.71	113113.69	243438.17	26779.07	103684.42	19778.45	16561.20	25485.86	5135.31	1492.63	4668.55	402.89	3761.26
28	xg9	3	564.58	132243.59	8650.11	9317.28	112070.95	241216.09	26369.56	102118.82	19433.90	16874.07	25952.29	6142.47	2007.22	5297.09	387.40	4015.84
29	xg9	3	4848.29	125918.64	6852.32	3968.13	109494.34	241188.17	27548.18	103086.33	17242.44	11108.50	44710.42	2147.39	1400.13	2492.00	50.00	4729.74
30	xg9	3	4300.81	125021.24	6578.24	4415.18	111722.21	244795.70	26533.77	103880.92	17953.58	11404.85	41548.74	2301.35	747.63	2426.28	527.71	4031.57
31	xg9	3	597.58	130726.63	9157.36	20255.02	113086.15	236047.58	25649.72	94781.64	16455.74	14105.12	24066.65	10148.34	2150.97	6991.26	1854.21	4860.12
32	xg9	9	15245.65	111962.37	12668.36	774.01	68938.94	188123.83	24287.11	108851.13	17881.23	7159.17	115637.40	2444.91	348.52	332.75	39.34	10687.70
33	xg9	9	16085.20	110459.37	12082.87	751.81	67341.71	183311.18	24536.95	105690.44	17665.51	6364.83	119050.80	2420.44	-75.08	441.01	211.83	10801.60
34	xg9	9	8771.65	121495.08	10108.22	496.21	86566.07	218832.58	26822.07	114366.61	19731.95	8882.02	74842.67	2036.05	765.04	372.83	-67.39	7317.71
35	xg9	9	8883.85	123255.48	10351.40	534.22	83896.03	218489.78	26936.79	114301.88	19596.84	7865.69	75798.79	1938.02	357.83	589.72	72.23	7465.35
36	xg9	9	900.04	133461.53	10099.53	20411.43	109271.79	230233.94	25255.32	94548.96	15530.42	14301.26	30643.52	9148.97	1880.28	7054.61	1983.01	5268.02
37	xg9	9	951.33	133694.40	10342.18	22416.58	104377.95	226255.27	24927.12	95988.44	17592.73	14368.71	29012.90	11606.07	2003.55	7659.15	2259.89	5630.34
38	xg9	9	1444.43	131693.28	8679.11	3765.71	111906.22	245883.77	26988.25	105587.98	19123.10	13914.95	31882.81	4578.18	1545.88	2537.13	-65.41	4186.04
39	xg9	9	1430.72	130871.73	8536.49	3392.69	112456.71	246535.72	27287.56	105710.16	20469.89	14882.76	31384.22	4342.57	1091.15	2371.36	215.60	3944.94
40	xg9	9	3409.14	129592.00	9867.58	928.26	99391.84	238243.87	27975.71	111584.52	19750.52	10969.27	47783.13	2163.10	453.80	296.45	9.39	4901.38
41	xg9	9	3734.39	127421.51	10189.42	823.69	99231.28	235887.58	27571.65	112013.71	20360.15	10641.55	50543.05	2223.54	97.16	381.97	-29.10	5279.28
42	xg9	9	7436.51	122934.32	11277.88	904.32	89592.98	219423.15	26142.02	108637.22	19247.36	9946.19	72176.96	2241.10	848.67	778.95	169.46	7203.79
43	xg9	9	3686.65	128729.78	9663.09	6632.14	102253.25	232525.52	26019.50	103698.22	19706.05	13435.08	46278.30	4512.66	1560.42	3291.59	431.95	5503.24
44	xg11	1	6057.27	121230.09	5465.57	1813.54	109575.09	250888.95	28585.39	107296.16	13622.61	4733.13	49425.71	818.18	157.27	743.43	219.48	3124.41

Table 1. Monazite Element concentrations in Parts per million as Measured on Cameca SX-100

spot#	sample	grain	Si	P	Ca	Y	La	Ce	Pr	Nd	Sm	Gd	Th	U	Tb	Dy	Er	Pb avg
45	xg11	1	6490.19	122556.35	5162.77	998.60	109405.24	252079.99	27743.63	108430.60	13650.75	5756.42	49587.23	726.59	607.04	347.16	-18.08	4066.33
46	xg11	1	3581.29	126686.15	7128.21	3876.74	120544.07	250379.67	27021.57	96220.53	15763.27	11056.45	37746.10	1258.37	861.02	2590.38	79.90	3140.82
47	xg11	1	3417.47	127476.76	6332.33	3941.11	122679.86	251779.71	26819.78	96924.41	15443.21	9827.83	37712.89	1033.85	1151.15	2175.64	115.01	3140.84
48	xg11	1	2226.21	128307.99	9071.21	17649.02	117789.34	234237.20	24794.10	91815.74	12686.71	10904.43	44024.82	1065.93	1198.51	6285.88	1416.93	117.90
49	xg11	1	2952.35	126941.93	8349.52	11586.23	113996.98	243582.37	26147.24	96935.56	14428.11	9360.76	42204.19	1275.21	674.33	4216.23	904.16	98.70
50	xg11	1	4065.72	126484.01	5964.63	5262.88	111687.93	242876.89	27744.70	103646.78	18462.59	13096.68	38994.70	3010.25	1417.67	3109.94	98.24	3498.48
51	xg11	1	3155.48	127702.99	7898.67	7008.98	115895.37	245596.64	26713.24	99006.73	13907.47	9504.29	44122.75	1569.66	651.43	2819.88	358.32	80.91
52	xg11	2	4951.12	124515.79	5376.55	3365.46	124515.67	253931.35	25991.74	97170.55	12649.40	7692.48	42205.13	1551.47	348.77	1385.75	288.43	3667.81
53	xg11	2	3256.56	127289.62	6935.09	2877.08	116839.03	247412.14	27858.52	102772.11	17884.89	11451.37	37565.61	3403.75	1343.47	2113.00	-64.22	3429.38
54	xg11	2	2651.85	128356.04	7638.16	5162.12	115792.63	242900.02	27602.95	102104.16	17850.14	13731.66	36518.10	4105.25	1604.11	3299.46	271.69	3565.99
55	xg11	2	8156.32	117370.38	4776.04	92.37	113510.10	247398.05	27199.08	103374.14	12527.66	4135.75	57576.24	892.69	96.85	139.24	19.89	4346.01
56	xg11	2	8097.55	119207.72	4992.77	646.71	112803.32	247024.26	27945.78	103681.33	12208.27	4788.63	58778.72	757.17	387.85	47.08	64.83	3855.58
57	xg11	2	6658.17	123171.78	5091.20	438.45	116472.21	249945.34	27867.55	103663.24	12462.82	4861.99	49550.76	657.72	240.54	265.33	248.37	4078.65
58	xg11	2	6598.77	119962.06	4920.82	450.08	116342.18	251034.18	27558.87	104840.46	12964.97	5054.25	49509.01	408.80	71.46	216.25	166.12	3790.84
59	xg11	2	6095.18	114019.35	5589.48	836.97	115732.85	249934.50	28379.99	104467.95	13154.80	5084.97	51692.44	915.47	613.33	721.87	85.39	3835.49
60	xg11	2	6826.62	122605.71	5563.25	480.75	115683.31	248927.62	28134.54	104038.16	12894.58	4376.70	52295.26	581.11	-2.95	219.81	171.20	3367.45
61	xg11	3	1126.45	131852.44	7301.04	21915.03	113642.01	240854.60	26250.04	94974.98	15843.15	12134.52	28733.95	3736.09	882.60	6941.41	2050.78	166.07
62	xg11	3	1615.57	128891.95	6287.28	15178.01	115963.25	249306.36	27098.68	99092.30	15602.63	11421.62	28093.18	2642.78	833.61	4674.61	1374.17	924.25
63	xg11	3	1473.72	131317.79	6443.97	9453.37	122748.50	254501.60	26983.20	97806.53	15369.21	9323.19	25295.74	2548.79	1088.27	3490.43	510.53	2537.64
64	xg11	3	1205.13	131321.50	6431.92	10126.78	124919.66	255648.67	27917.60	97315.45	14631.03	9504.95	24814.78	2613.67	1445.96	3413.98	953.15	2225.94
65	xg11	3	1876.40	128859.53	5562.07	15223.30	109120.95	252479.99	26986.90	101268.50	17833.83	13451.01	24227.55	4270.38	1290.86	5109.10	1276.77	2642.26
66	xg11	3	2904.55	126477.29	4821.42	4208.02	122359.68	261915.07	27674.36	101498.18	15483.47	9119.83	29110.53	1079.45	657.26	2186.92	429.12	2423.98
67	xg11	3	2723.46	128856.47	4867.87	7804.05	118254.64	257763.43	27760.29	103184.50	16573.11	10863.31	27909.11	1857.08	792.91	2937.96	567.10	1865.61
68	xg11	3	2253.23	128271.42	6080.36	11942.58	111220.75	247850.82	27191.82	102431.23	18002.98	13711.06	27333.52	5325.08	1175.85	4595.23	1052.39	3226.17
69	xg11	3	1891.58	128123.30	4902.28	10642.76	113711.33	257929.40	28588.52	102604.42	18518.76	12930.47	22548.30	3673.48	884.12	4076.53	1084.28	2276.96
70	xg11	3	2131.55	129577.16	5005.53	8662.22	113243.64	256817.85	28945.37	104420.36	18289.94	12409.81	24249.16	2899.61	1330.46	3616.96	755.21	2421.59
71	xg11	4	3342.47	126534.41	4666.34	670.69	107584.43	268479.02	30142.30	118580.39	16307.34	5696.98	30240.34	1956.60	664.56	254.34	-74.25	2859.30
72	xg11	4	2977.64	126180.48	4597.15	919.78	107889.18	266051.69	30469.71	116372.29	16104.03	5709.11	29003.94	1961.96	-11.82	200.96	117.74	2273.16
73	xg11	4	3171.27	128411.33	4397.97	501.08	107079.91	268498.23	30703.48	116856.86	16330.67	5271.13	28590.23	1713.87	569.48	343.38	121.67	2874.99
74	xg11	4	1799.46	129822.12	4330.13	1727.45	123900.89	272353.78	29767.46	102716.56	15406.43	7837.16	19027.69	5183.05	338.14	993.70	260.04	2063.86
75	xg11	4	5062.19	126032.76	5164.59	508.78	101074.43	255588.65	30950.15	117191.66	15720.34	5050.59	41690.64	735.25	451.32	63.91	149.73	3499.92
76	xg11	4	4808.72	124174.52	5119.95	673.46	100103.74	257938.20	30394.36	119640.92	16852.82	5395.50	40781.51	738.44	303.17	206.61	-181.56	3324.29
77	xg11	4	4225.73	127124.75	6722.03	6004.86	106539.65	245471.05	27681.48	106109.68	18013.08	12616.50	41112.53	3253.06	938.93	2948.42	123.60	4197.18
78	xg11	4	5540.76	125411.09	5332.12	703.51	99854.93	252982.28	29967.79	114223.78	16383.21	6612.28	43851.63	993.60	594.98	297.49	213.86	3816.53
79	xg11	4	2262.05	130923.19	11700.23	9724.17	112061.66	231145.53	24345.90	90524.23	17295.47	13844.35	44040.34	5986.86	1598.74	4197.20	380.16	5502.13
80	xg11	4	2389.53	129363.80	12272.84	9658.02	110090.53	227908.55	24165.12	92623.70	16716.02	13670.83	47630.99	6851.47	1534.62	4694.58	508.44	5971.36

Table 1. Monazite Element concentrations in Parts per million as Measured on Cameca SX-100

spot#	sample	grain	Si	P	Ca	Y	La	Ce	Pr	Nd	Sm	Gd	Th	U	Tb	Dy	Er	Pb avg
81	xg11	4	8897.61	113797.61	6601.40	498.97	92456.44	234972.83	28386.71	113825.88	16186.89	5421.93	68766.93	1282.80	286.70	149.12	98.23	5570.03
82	xg11	4	8502.16	116759.93	6186.88	366.93	93105.67	237322.20	28826.63	112692.99	15913.21	5569.62	64349.08	1416.98	332.33	301.79	90.10	5282.32
83	xg11	4	2033.42	127677.77	5446.56	2543.84	120360.24	262323.95	27547.18	103273.06	17389.75	10215.16	25406.06	3205.66	768.83	1351.69	322.53	2766.34
84	xg11	4	2270.36	127807.25	5491.95	2136.33	118511.89	262159.34	27198.31	102637.34	16890.54	9491.95	24983.69	5352.96	954.88	1355.28	240.71	3206.38
85	xg10	9	24639.03	95106.24	2106.25	855.27	73474.86	195050.30	24984.44	103169.58	14766.71	6435.28	130777.32	1912.58	342.60	277.58	-269.93	8400.22
86	xg10	9	6774.40	121697.58	3534.97	414.90	107297.25	254762.09	30161.44	118368.28	14870.01	5154.27	43968.88	511.87	627.05	183.22	75.70	4219.96
87	xg10	9	7523.87	121174.89	3615.52	440.75	104660.78	253579.93	29736.70	116097.51	14074.79	4857.61	47793.82	575.21	318.31	281.93	146.29	4588.55
88	xg10	9	7601.16	121889.95	3592.07	569.49	103805.80	251423.17	30364.43	116759.04	14568.49	6278.55	48505.22	461.97	-202.62	141.26	165.40	4411.55
89	xg10	9	2434.38	128885.23	3979.41	114.21	119175.02	266983.26	29842.56	111685.78	20649.02	8918.79	22339.93	2103.50	318.95	161.58	237.28	2626.62
90	xg10	9	3068.87	128326.14	5120.39	2305.86	117585.55	252931.05	28394.41	107951.26	20137.38	12947.03	29673.35	2282.10	737.83	1793.73	187.86	3358.68
91	xg10	9	3727.17	126564.05	2943.23	1850.87	112638.41	261493.13	30353.45	115065.87	18921.65	10266.33	25797.14	1059.76	685.39	1156.48	149.86	2779.32
92	xg10	9	9773.81	118564.40	3254.92	443.13	103335.47	245198.77	29682.19	112622.94	15328.65	5302.86	57497.25	877.63	169.33	501.83	-114.90	5588.51
93	xg10	9	8254.18	120171.32	3388.98	477.37	102830.94	251662.40	29106.63	112852.88	14564.47	5435.95	50685.58	659.76	398.36	541.73	270.55	4910.50
94	xg10	9	8325.59	119768.42	3657.37	722.95	104873.44	245834.08	29334.84	111366.07	15111.90	7978.46	52581.71	1035.80	423.61	449.64	163.65	5172.49
95	xg10	9	1419.22	131727.23	8073.12	15426.07	119361.16	238971.73	25616.96	95065.08	15530.46	13386.14	24799.90	8936.09	1379.42	5804.55	836.59	4550.59
96	xg10	9	2706.40	126668.92	7687.95	11377.21	115397.24	242601.11	26410.41	103338.73	17183.99	11928.89	28444.27	8709.83	1027.15	4487.40	1060.05	4704.35
97	xg10	9	9086.87	114407.63	4083.18	917.19	96019.17	240458.95	29231.16	120851.93	15265.84	6325.37	60359.00	920.32	256.61	472.35	195.01	5816.03
98	xg10	9	9812.52	116234.19	4132.89	1063.71	92013.39	237603.61	30434.69	119603.37	15432.80	6683.34	61047.94	635.89	511.10	652.99	330.02	5019.83
99	xg10	9	2965.39	127148.27	5254.63	2394.88	116238.23	251391.32	28745.51	105290.31	20392.38	13597.92	28499.05	2464.40	1199.50	1736.59	-62.49	3320.50
100	xg10	9	3034.83	126212.04	5759.33	3144.40	115330.31	249470.80	27941.14	106380.26	20989.85	14997.73	29813.33	2931.30	927.76	1909.85	206.40	3517.75
101	xg10	9	9825.31	116864.36	3415.75	438.94	101719.65	243544.98	28990.48	113078.71	15401.15	6001.70	58560.50	843.88	403.71	267.67	65.95	5555.59
102	xg10	10	2455.93	128805.11	3432.08	1623.44	109807.78	274700.94	31275.26	117679.32	16159.11	8170.61	21482.39	1073.39	408.82	947.72	18.07	2301.74
103	xg10	10	2136.41	126965.15	3557.23	1686.55	113111.82	275671.28	31317.51	112835.65	16027.59	8325.20	20248.04	1269.28	469.00	1062.11	54.03	2144.35
104	xg10	10	3880.27	125083.48	3888.06	1494.10	104570.14	261196.35	31499.07	119933.11	17162.58	8041.37	30116.06	825.59	783.55	950.78	-35.01	3020.41
105	xg10	10	4181.74	123945.10	3952.43	1389.20	102062.34	262643.61	31058.34	121601.16	16745.04	8194.49	32216.01	796.53	779.21	738.21	48.19	3185.59
106	xg10	10	9816.12	115191.69	3970.44	778.85	89884.26	237352.51	30102.39	121330.50	16301.77	5988.66	61213.47	760.76	234.90	412.21	-20.64	5721.49
107	xg10	10	10035.88	113428.19	4334.54	542.85	87299.03	233553.31	30195.42	127667.75	16437.57	5361.06	63500.16	892.25	4.12	187.14	-131.05	6027.39
108	xg10	10	7064.50	118337.47	3856.84	630.16	93039.75	245650.34	32039.37	125461.11	18694.59	6581.79	46445.35	863.32	786.00	561.96	80.83	4477.08
109	xg10	10	7040.94	117943.57	3636.53	521.21	93881.26	247966.94	31662.22	128326.10	17894.78	6220.00	45553.72	891.07	638.13	303.30	201.33	4518.59
110	xg10	10	1745.11	125390.05	5332.53	1585.99	104900.21	265516.96	30677.16	121058.46	18716.45	8249.09	24238.74	562.93	325.43	879.36	-156.45	2482.02
111	xg10	10	1336.55	127867.74	5017.34	1611.51	105667.70	268676.76	32208.76	118512.83	18988.93	8232.25	20211.14	632.44	157.65	590.05	272.18	2051.02
112	xg10	8	4151.97	124942.30	3153.75	1663.17	114700.86	256187.24	29297.77	115131.54	21581.47	11874.30	28549.93	1402.64	1122.97	1307.48	173.90	3095.54
113	xg10	8	4038.39	124462.24	3276.17	2077.61	114654.05	253878.33	29467.47	113794.59	22183.99	13580.39	28979.87	1583.40	1236.06	1545.21	50.99	3035.12
114	xg10	8	6171.68	122558.79	3379.64	792.89	103185.74	257954.93	30303.56	120054.42	16048.77	6581.04	40158.45	539.29	622.57	607.01	89.66	3835.26
115	xg10	8	6591.70	121382.05	3471.63	298.05	107277.56	256690.98	30217.15	117010.16	14832.83	5623.52	42327.55	535.82	627.62	-25.90	-5.94	3974.03
116	xg10	8	2117.95	126583.07	6214.01	10595.56	115609.56	240816.35	27030.76	102772.03	20078.16	17899.76	26896.14	4216.31	1914.61	5690.73	498.76	3507.73

Table 1. Monazite Element concentrations in Parts per million as Measured on Cameca SX-100

spot#	sample	grain	Si	P	Ca	Y	La	Ce	Pr	Nd	Sm	Gd	Th	U	Tb	Dy	Er	Pb avg
117	xg10	8	2719.85	125341.09	4872.09	3075.05	114353.91	249328.65	28985.78	110678.82	22280.31	15069.33	28184.35	1999.97	819.75	2258.33	225.56	2054.10
118	xg10	8	2302.04	126192.75	5880.32	7250.80	116139.67	248124.29	27360.96	103541.84	20091.07	16307.63	27115.43	3685.23	1029.49	4383.48	278.72	3395.60
119	xg10	8	2302.90	125461.06	6034.75	7623.91	114839.51	242933.41	27458.42	105196.86	21638.65	16505.74	26916.01	3904.53	1671.10	4016.70	129.77	3432.49
120	xg10	8	5153.80	120188.73	3650.26	386.54	102480.15	257513.35	31640.31	123721.21	17833.33	6581.06	36733.01	1006.25	591.18	230.81	72.07	3379.72
121	xg10	8	4952.09	121769.37	3527.68	423.81	102634.91	256970.08	31694.42	122964.09	16956.71	6158.79	34977.80	895.62	242.98	195.14	-47.89	3312.24
122	xg12	2	962.33	126235.38	8412.69	23906.19	106920.45	232732.56	26078.64	99701.36	15511.75	14806.64	33625.42	2513.08	1255.03	7270.07	2339.18	144.14
123	xg12	2	1318.47	127903.22	8695.50	23195.84	106812.25	230538.40	26335.28	99519.17	16534.12	13108.95	36130.46	1862.12	1668.24	7019.36	2117.90	222.22
124	xg12	2	3377.70	124466.04	7263.62	1987.06	113700.67	247188.53	27906.73	107248.49	17655.91	10702.39	38798.28	2379.01	1240.18	1403.72	125.84	4151.64
125	xg12	2	3326.96	124179.67	7403.50	2410.79	112271.59	245851.92	28478.00	107469.77	17056.65	12145.80	39102.27	2202.38	810.24	1704.93	324.13	4199.58
126	xg12	2	1766.46	124801.77	10838.93	6805.24	108125.54	236932.02	27314.57	101383.38	18001.74	12739.00	36832.48	10923.59	1293.24	3004.36	330.27	5084.22
127	xg12	2	1086.75	126878.48	12152.29	9999.92	105084.05	232413.07	26594.61	99336.47	17567.47	12863.53	38286.73	12601.74	1556.46	3982.29	640.62	4073.20
128	xg12	2	6254.61	117509.77	8996.85	1562.04	90873.87	228356.97	28371.09	114217.01	19138.11	8450.98	60581.59	1326.73	498.01	749.30	49.79	5931.82
129	xg12	2	5688.95	117788.38	9207.95	1504.38	93941.63	233483.90	29110.68	114247.01	17577.11	8597.47	58703.32	1577.30	1062.16	957.41	148.61	5851.48
130	xg12	4	1678.74	126258.95	6170.25	21465.01	115041.42	239499.80	26879.21	99446.72	14845.36	12675.87	30253.37	543.42	1675.84	6574.19	1911.16	97.77
131	xg12	4	1454.35	127358.62	8139.06	19907.01	111572.99	238338.22	26962.57	99403.77	15317.15	13201.82	34672.13	2374.76	1741.14	6041.51	1794.90	161.96
132	xg12	4	1651.84	127657.69	7994.44	20951.03	109642.37	235407.15	26222.18	97753.46	15092.68	12102.81	36374.09	1210.07	899.30	5963.38	1980.11	159.46
133	xg12	4	3556.94	122638.92	6397.80	2378.38	114515.23	251413.95	27828.18	105227.98	16253.89	10145.53	38383.27	1509.62	890.96	1278.15	68.53	3625.43
134	xg12	4	3988.27	120473.05	6393.63	2430.53	114152.85	249602.12	27792.66	106126.91	16420.41	9573.85	40322.02	1537.44	783.36	1290.06	312.61	4053.11
135	xg12	4	22322.79	85043.20	7545.45	11015.97	86793.14	182011.79	19765.42	69758.39	11691.40	11593.68	148532.45	6534.10	1293.26	4591.15	1004.36	87.05
136	xg12	8	1304.67	127941.53	11626.03	17163.00	105711.11	231724.06	26179.22	96414.97	15110.98	11599.58	42837.87	6048.91	1288.23	4469.46	1669.74	103.98
137	xg12	8	1000.66	127416.05	8217.58	22271.70	107385.08	235766.94	27197.03	97811.94	16045.65	12089.19	32740.90	2750.76	1639.80	6363.74	2168.05	120.25
138	xg12	8	1754.61	126845.75	8555.25	21194.01	110688.26	236527.84	26724.23	97525.41	15603.73	12149.30	36786.47	2268.06	2016.50	6330.72	1989.12	137.65
139	xg12	8	1427.31	127922.68	8253.06	21033.10	107565.50	236187.52	27035.07	99867.42	16229.95	12593.24	35116.24	2058.92	1561.11	5612.60	2255.25	149.25
140	xg12	8	9143.16	111793.48	6136.56	1168.86	97557.23	234414.02	27896.08	111333.92	16433.75	7588.19	65868.83	1550.60	237.03	624.10	55.12	5939.61
141	xg12	8	9087.04	110093.96	5928.22	612.78	95764.99	234344.61	28488.93	111469.04	16249.64	8233.31	65806.89	1331.37	308.88	579.18	-15.89	5984.53
142	xg4	5	2901.76	125243.07	6525.77	8601.42	97282.84	233559.37	28903.40	116509.29	23381.52	17531.22	31028.77	5591.76	1810.61	4321.96	350.73	4281.10
143	xg4	5	2673.60	124146.50	6279.18	9369.54	99381.44	233902.26	28769.66	115942.16	23880.57	18895.82	28836.58	5659.94	1551.51	4470.10	503.12	3956.41
144	xg4	5	1422.42	127383.54	5660.75	23552.63	105973.90	227792.01	26777.95	103886.58	21290.36	22180.51	21231.31	5084.83	2996.98	10499.43	1580.57	3261.01
145	xg4	5	1415.17	127604.28	5235.95	22176.95	109053.76	232723.17	26428.40	103166.67	21496.87	21479.97	20228.79	4723.21	2393.94	10194.66	1301.44	2995.63
146	xg4	5	13634.71	108265.92	7132.30	2449.57	67872.39	199648.91	27785.50	125440.96	22710.29	9482.22	88500.52	2429.03	544.55	956.60	358.94	8382.09
147	xg4	5	10087.43	119294.91	8195.60	5524.02	70606.25	208333.16	28943.95	124061.32	22449.20	12747.67	61004.19	3765.81	1102.93	2469.35	523.07	4598.82
148	xg4	5	2176.85	124921.44	5964.91	11757.97	102511.53	230951.64	27906.94	112003.25	24023.32	20998.57	26241.48	5410.42	1728.75	5836.00	553.31	3409.71
149	xg4	2	15335.68	106625.19	6139.07	1134.45	73952.41	203300.92	27571.32	118538.98	20567.27	7697.75	96665.58	2578.69	192.30	766.47	291.41	8742.11
150	xg4	2	15602.79	106512.86	6163.26	1136.30	72764.49	205550.57	27865.88	119339.14	20036.82	7728.72	94815.39	2426.00	825.30	510.00	301.31	8787.72
151	xg4	2	4827.44	121730.61	7844.39	1989.75	99074.31	233382.13	28137.51	115395.77	21293.16	11759.58	48579.03	2465.16	590.73	1181.24	239.98	5178.93
152	xg4	2	4386.42	122252.34	7900.00	2072.08	102166.45	239829.19	28631.85	112709.96	20716.59	11051.84	46613.81	2301.52	1042.45	1126.45	233.06	4915.70

Table 1. Monazite Element concentrations in Parts per million as Measured on Cameca SX-100

spot#	sample	grain	Si	P	Ca	Y	La	Ce	Pr	Nd	Sm	Gd	Th	U	Tb	Dy	Er	Pb avg
153	xg4	2	1559.43	127414.39	4491.78	15159.71	119669.32	249146.11	27026.38	102419.06	18685.02	14197.98	23081.25	611.14	1425.60	5855.18	1372.35	587.76
154	xg4	2	1028.86	129711.05	4465.72	17159.44	123005.92	247820.00	27122.83	98210.94	17706.68	14805.95	21001.17	247.81	1647.28	6474.36	1628.45	64.15
155	xg4	7	4473.00	124376.23	6027.16	21772.45	99825.51	220496.53	26784.33	104968.89	20488.18	19940.13	38338.21	4161.67	2398.25	9464.61	1488.87	4738.30
156	xg4	7	4511.45	123004.72	3624.02	8320.08	103259.49	235639.30	28434.04	116193.28	23954.86	18001.33	31452.91	3545.05	1295.16	5045.08	326.38	3668.41
157	xg4	7	1566.05	128864.72	7552.18	22848.33	104025.11	225991.45	25957.69	99931.38	20457.99	19827.16	28029.08	5710.53	2433.64	9640.81	1627.73	4082.43
158	xg4	7	1904.62	127159.66	7682.12	24000.29	101061.30	222847.02	25304.82	102828.36	20349.57	21672.62	29605.67	5797.32	2721.34	9964.22	1735.57	4398.48
159	xg4	7	10753.14	114355.56	8863.65	3824.18	81713.04	205091.91	27283.81	115211.10	20888.43	11213.79	79094.46	4880.25	575.97	1914.90	126.79	8391.86
160	xg4	7	9336.25	112975.11	8689.61	6679.20	84858.80	207820.80	26890.32	112283.95	21665.22	13857.62	69400.80	5192.62	1062.35	3263.64	429.90	7783.84
161	xg4	7	23393.66	88066.18	6450.19	1953.32	58771.57	171115.71	23499.72	106939.51	19761.17	8125.13	143300.83	3499.24	220.65	834.40	331.96	11493.32
162	xg4	7	25200.69	92480.61	6257.50	1887.42	59393.08	170941.62	24680.98	109198.61	19093.81	7670.84	142695.97	3442.52	872.45	896.90	103.58	11543.58
163	xg4	7	13405.60	107188.38	6852.08	2482.37	76608.20	204524.57	28099.71	118075.24	22456.88	10259.67	87398.08	4225.92	742.89	1452.39	71.91	8547.94
164	xg5	1	2528.95	124439.73	8773.02	10217.80	114271.28	252487.16	26666.37	93743.57	12979.68	7935.79	39843.30	2514.07	414.46	2374.07	658.41	4358.84
165	xg5	1	2793.50	125094.21	8849.71	10396.08	114954.79	249188.54	26670.94	94196.59	13178.26	7720.00	40974.47	2548.39	958.99	2552.93	620.48	4474.64
166	xg5	1	6960.85	119695.80	3640.42	4388.34	119494.94	257495.59	27172.47	94359.74	12013.83	6118.16	45514.97	951.80	699.93	1508.21	270.28	4355.62
167	xg5	1	7800.80	119046.81	3419.37	3832.87	122455.26	255156.63	27037.63	93879.89	11302.68	6040.28	48688.03	718.37	483.15	1251.75	240.13	4658.42
168	xg5	1	10021.13	114521.97	3706.47	3719.65	113422.10	245983.49	26078.83	93567.81	12826.06	6402.99	60865.45	1068.70	9.63	1406.91	291.14	5929.34
169	xg5	1	4896.92	121649.35	6518.96	4731.71	109359.02	252777.45	28146.64	97717.71	16184.72	9553.66	43853.41	1255.50	779.68	1849.29	127.60	4457.86
170	xg5	1	5344.55	121005.69	6363.65	4098.99	105158.40	243927.65	28757.78	102673.26	19106.65	11947.80	46028.27	1599.03	990.61	2243.64	219.35	4777.30
171	xg5	1	77043.46	16665.26	2546.83	9405.07	11683.20	25589.80	2504.22	11554.02	1753.81	2582.77	388485.44	45149.85	464.52	2328.88	598.01	347.79
172	xg5	3	15876.79	78689.70	9623.41	14424.90	63056.67	146766.60	11940.75	29674.21	3808.06	5010.34	131358.10	139732.42	864.51	5027.79	1655.02	1912.22
173	xg5	3	992.94	128963.52	14697.96	22377.85	168538.53	214573.78	15638.21	39330.75	5747.05	6934.43	39374.38	20269.71	1479.31	6482.82	1964.36	7130.80
174	xg5	3	572.93	129404.30	9126.84	19214.13	180120.07	235211.80	18168.66	46081.02	6883.06	6875.92	20222.02	17466.04	1076.77	5627.08	1610.61	4882.61
175	xg5	3	474.10	127235.81	9267.84	15851.04	195499.35	237948.20	17305.41	41110.10	5806.96	5967.50	19150.92	15838.54	1121.27	4786.09	1215.03	4674.47
176	xg5	3	2055.36	125924.00	11872.64	3687.31	181025.36	232009.91	16285.49	42302.29	5983.36	5538.68	54898.89	760.81	765.94	3009.16	314.28	1073.64
177	xg5	3	977.35	130173.95	13440.53	20234.49	173964.70	219659.73	16534.00	39797.77	5583.95	6900.23	38204.30	15981.85	665.62	6000.49	1514.40	6098.70
178	xg5	4	25872.79	92933.39	1376.65	532.89	114333.61	209838.14	19186.00	62942.06	5128.57	1596.32	133354.73	2576.85	-19.31	24.31	-261.07	7170.33
179	xg5	4	21285.78	102094.37	2173.85	720.56	124362.53	223001.81	20233.13	67310.10	5121.25	1845.08	106424.37	1898.05	104.86	256.40	76.88	6949.13
180	xg5	4	2812.38	126187.90	3085.73	2047.59	162986.76	281104.46	24613.19	77299.49	7512.76	3104.54	22196.14	717.66	412.42	808.32	235.68	2293.15
181	xg5	4	1047.95	127146.00	8680.60	2620.77	155524.23	269129.18	23608.69	74746.74	7053.53	3022.21	32391.84	1117.51	628.57	551.63	598.46	3272.89
182	xg5	4	3039.90	125526.26	6309.00	4093.40	127836.24	255169.09	26329.35	95336.18	15033.70	9809.22	34155.45	1235.06	1004.12	2242.36	322.59	3394.68
183	xg5	4	3251.90	125060.48	6281.57	4654.91	125985.76	254170.41	26515.16	94828.11	15194.09	9238.41	35255.70	1291.67	637.92	2406.91	274.31	3655.04
184	xg5	4	7873.95	117636.72	404.51	2286.64	133794.99	266159.78	27255.55	94115.83	12922.73	7390.44	36546.91	1254.47	489.08	973.10	298.72	3585.93
185	xg5	4	4612.42	123350.75	3843.65	1279.85	112963.02	265466.50	30041.63	112289.09	13784.10	5568.15	34087.40	700.34	310.80	444.67	180.03	3303.42
186	xg6	10	10459.42	113648.84	4490.60	62.05	94127.43	238078.41	29843.76	115966.34	14308.75	3969.96	65825.01	975.14	723.38	216.47	-215.00	6275.69
187	xg6	10	13778.27	107685.28	3705.07	-191.43	84339.42	228784.80	29617.99	121683.30	12173.14	1612.08	81425.21	1320.81	185.16	-271.19	134.37	7397.43
188	xg6	10	6182.45	119021.81	3409.95	-168.21	102043.32	257459.73	31400.39	123688.46	14356.99	3539.94	41325.34	646.48	-113.00	-237.63	130.08	3936.66

Table 1. Monazite Element concentrations in Parts per million as Measured on Cameca SX-100

spot#	sample	grain	Si	P	Ca	Y	La	Ce	Pr	Nd	Sm	Gd	Th	U	Tb	Dy	Er	Pb avg
189	xg6	10	6919.43	117909.48	6626.29	390.55	100135.21	234237.54	27878.78	115366.88	19285.00	8615.06	55870.51	1501.99	511.23	363.62	-9.51	5496.56
190	xg6	10	2600.09	125382.59	7086.55	6147.01	109837.71	240905.40	28262.27	106045.72	20700.52	14790.13	33108.82	3217.89	1075.61	3195.32	326.58	3947.81
191	xg6	6	12846.90	108110.87	3594.96	-176.49	86188.00	229602.56	29988.30	121007.45	12722.52	1847.01	75332.80	1302.04	-5.80	-376.94	103.81	6667.91
192	xg6	6	2923.56	123984.68	5604.76	2548.53	110127.54	242160.64	28427.91	109490.37	21180.13	14446.28	31745.35	1947.24	1241.90	1854.89	86.19	3421.14
193	xg6	6	3257.56	124201.10	6243.99	1159.51	109485.73	247747.08	28355.54	109821.82	20681.14	11606.55	35936.66	1515.53	821.34	1023.46	101.22	3762.92
194	xg6	6	10521.11	115050.42	3414.62	-181.67	91579.29	239752.18	29549.02	119744.23	13046.77	2989.45	64207.64	849.85	257.50	31.25	296.84	5706.46
195	xg6	6	4882.97	123174.57	3893.98	930.00	106052.69	246525.39	29191.99	118293.43	19351.90	10255.51	36091.90	995.46	210.33	870.93	-19.78	3524.65
196	xg6	6	1984.51	127076.04	6704.74	6897.43	111960.70	239203.02	27647.38	103997.43	20172.55	16741.66	28888.08	3442.37	1404.29	4440.29	155.22	3616.12
197	xg6	6	9173.53	113548.95	3298.65	-183.74	93576.00	244824.39	30092.11	119551.85	13107.85	3549.19	56411.46	1054.30	-53.12	37.20	-159.33	5409.72
198	xg6	6	12993.60	108618.80	3581.41	-216.70	83848.50	228942.84	30241.03	121570.98	11899.21	2612.54	75675.94	1068.23	343.91	-336.72	9.45	6879.35
199	xg6	6	6029.51	118495.71	4455.40	769.78	95678.70	247736.67	30442.85	120142.13	16287.39	5520.03	44565.65	947.70	399.42	217.33	202.87	4486.97
200	xg6	7	1542.75	128216.08	8238.35	6515.74	110574.42	239635.04	26721.81	103988.95	19944.56	15791.16	33058.08	2878.77	1350.66	3791.62	282.33	3768.00
201	xg6	7	1484.97	128945.67	8175.88	6848.63	113045.90	239101.08	27834.57	104218.54	19888.41	16070.94	32313.39	2753.63	1142.72	3984.74	414.15	3780.65
202	xg6	7	4600.70	122183.26	4111.40	756.96	102711.05	259095.17	31908.69	118212.76	15577.03	5214.88	35724.45	963.44	357.02	267.39	118.86	3595.34
203	xg6	7	5941.77	122127.05	3901.44	-145.98	100164.96	255822.33	32103.63	122718.71	16831.73	3702.46	41122.71	620.99	852.47	-234.23	81.17	4112.63
204	xg6	7	6913.60	121763.61	5558.91	828.28	96231.57	245515.02	30110.48	118320.52	16250.43	6736.70	51668.21	957.50	347.30	637.44	166.57	5036.77
205	xg6	7	8888.55	115819.03	1297.62	1047.92	98868.22	247696.97	30180.22	121781.20	18113.98	7899.91	53687.63	641.26	121.18	596.64	-159.70	373.64
206	xg6	7	6901.71	118509.33	2183.39	548.11	100772.58	251020.69	31677.92	125927.16	17270.31	6464.65	45886.45	617.29	627.45	216.49	147.54	278.46
207	xg2	1	22853.59	97282.23	2848.17	1408.53	122678.07	218430.70	19258.59	59477.98	4398.68	2489.65	117860.11	2540.84	331.63	400.80	1.24	10958.32
208	xg2	1	22167.86	99579.46	2963.51	1366.25	126001.54	217504.85	19201.36	58895.24	4591.29	1848.02	114347.52	2468.66	248.91	428.28	-83.86	10298.42
209	xg2	1	23133.86	95559.06	2904.44	1372.59	121033.43	216941.77	19172.89	59110.48	4970.35	2030.76	120445.71	2670.91	316.37	517.95	2.33	10622.91
210	xg2	1	26158.77	91624.51	3161.77	1332.20	117270.82	206149.59	19016.69	53291.47	4861.83	1651.87	136164.54	2327.01	138.98	245.48	42.04	8009.93
211	xg2	1	25695.13	91013.97	2852.56	1247.16	117692.56	208166.67	18194.95	54854.43	4451.76	2099.37	136063.84	2275.72	13.07	232.87	108.96	7855.34
212	xg2	1	40927.89	69065.17	5603.84	1001.52	99327.38	144966.72	13948.40	42850.82	3631.34	1522.08	215709.58	4432.17	68.18	370.93	91.17	6024.57
213	xg2	1	50892.72	54910.95	3963.58	818.92	80797.88	117965.90	11394.31	37130.35	3642.46	1937.14	263615.50	5060.73	60.43	501.40	-44.29	8289.70
214	xg7	1	4796.82	121123.83	6005.33	3796.22	139538.78	286835.28	27448.34	86221.04	8743.07	3424.47	18887.42	291.25	121.81	1019.72	416.67	27.45
215	xg7	1	4993.17	121167.90	5326.88	3617.44	138900.13	287477.16	27490.57	87921.50	8642.01	4192.11	20168.20	27.96	202.99	994.69	148.16	41.22
216	xg7	1	4488.22	122237.03	5112.09	3296.71	141742.27	288044.08	27012.43	86698.32	8951.20	3670.85	18482.83	204.71	321.33	1051.28	168.54	79.31
217	xg7	1	3699.07	124066.81	4831.86	2842.23	152226.08	292950.22	27574.29	82297.12	8350.64	3274.16	10906.09	236.25	375.08	848.45	115.15	10.65
218	xg7	1	3863.28	123267.17	4629.87	3040.28	147520.42	291410.50	27086.36	83631.82	7548.64	3378.48	12720.37	-49.53	254.97	922.67	475.18	35.47
219	xg7	1	3749.62	122484.43	4854.39	2940.90	148762.34	289830.13	27151.97	83881.37	7199.30	3807.91	11953.81	13.30	53.21	940.49	382.57	46.12
220	LSG	1	7304.02	121801.84	3422.32	7345.25	144729.95	267870.10	25495.84	81885.52	9260.08	5311.22	34455.20	1757.54	125.51	2181.71	469.89	78.23
221	LSG	1	8003.33	120642.68	3851.88	8334.16	135272.59	260678.95	25496.90	85530.53	10708.24	6945.39	41279.33	1833.04	682.36	2380.82	952.07	64.59
222	LSG	1	7561.91	120302.20	4017.86	7966.19	138331.05	263771.47	25676.93	83690.29	9640.56	6301.56	38823.05	1717.01	568.07	2290.95	904.31	55.27
223	LSG	1	7273.90	120967.77	4318.12	7798.27	138239.30	264251.22	25458.14	84705.39	9933.50	5801.87	36938.81	1877.08	664.45	2214.23	576.87	9.16
224	LSG	1	8043.05	118551.66	3438.02	8042.35	135523.28	260314.90	26017.36	86766.40	10407.14	5861.85	43955.74	1717.97	409.90	2510.92	689.32	48.74

Table 1. Monazite Element concentrations in Parts per million as Measured on Cameca SX-100

spot#	sample	grain	Si	P	Ca	Y	La	Ce	Pr	Nd	Sm	Gd	Th	U	Tb	Dy	Er	Pb avg
225	LSG	1	7787.97	119322.63	3438.07	8147.55	136136.61	259586.36	25933.52	86527.54	10487.70	6687.42	41831.59	1802.84	1412.56	2235.46	558.61	39.43
226	LSG	2	7075.01	121849.06	3864.19	8641.39	139992.23	259134.61	26647.23	85847.06	9886.96	6792.97	37455.44	1811.65	388.07	2601.40	718.72	63.19
227	LSG	2	6312.08	122736.59	4803.31	8781.65	140919.09	260150.63	26047.08	87349.05	10332.79	6501.89	32693.70	1358.41	781.63	2616.71	665.94	77.52
228	LSG	2	6533.12	122118.93	5333.20	8745.03	140729.37	261623.84	26095.48	87887.20	11046.99	6931.79	32670.64	1479.59	828.21	2582.44	714.52	77.44
229	LSG	2	6647.62	119457.52	5030.06	8916.65	140322.99	260200.23	26018.09	87468.05	11281.44	7252.73	34089.34	1610.68	479.36	2697.63	820.37	52.55
230	LSG	2	4421.82	123696.17	4228.43	7449.32	156365.14	270668.23	25853.71	85521.95	9649.94	5650.20	18349.69	845.95	370.15	1921.34	715.17	57.20
231	LSG	2	4514.26	125893.59	3996.62	7986.77	153225.76	271691.33	25433.32	84929.98	10541.53	6441.65	20694.93	984.68	310.18	2202.23	933.50	53.64
232	LSG	2	11924.27	110120.37	3037.77	7511.53	128888.19	242884.06	25187.50	85947.03	10648.54	6367.63	65378.88	1939.45	573.56	2170.43	565.14	115.26
233	LSG	3	6828.14	121134.91	3915.92	8965.14	138283.64	260953.53	26457.73	86718.64	10684.62	6385.82	35483.04	1691.42	819.02	2299.91	809.94	96.64
234	LSG	3	5703.47	120073.30	3616.09	7691.17	146535.84	267668.00	26179.05	85886.07	10536.01	5687.14	27475.51	1471.33	816.06	2300.57	840.92	95.67
235	LSG	3	4047.64	125591.59	4078.47	7590.33	154325.20	272627.00	26850.73	83026.03	9827.42	5664.49	17904.63	669.52	330.57	2084.94	896.25	39.04
236	LSG	3	5256.14	123668.46	3365.72	7866.38	140827.09	268740.79	27599.43	88706.40	9796.42	6069.21	26039.53	1531.27	558.56	2354.18	789.04	32.57
237	LSG	3	7394.05	121163.15	3010.85	7638.48	136834.44	258709.26	25538.62	87156.75	10926.34	6269.32	39536.32	1946.84	689.90	2342.50	692.15	89.75
238	LSG	3	6015.50	123234.49	3208.56	7978.70	139265.93	266556.80	26880.52	88541.70	10444.84	5983.03	29824.50	1754.64	40.77	2327.92	650.18	127.33
239	LSG	3	5349.46	123382.30	3129.79	8043.89	140851.56	267545.83	27254.34	90571.39	10341.00	5606.85	27188.76	1395.89	594.31	2358.20	607.21	16.99
240	LSG	3	5457.07	122949.73	3143.60	8502.26	139134.19	266685.89	27080.18	89544.03	10704.28	6811.53	27881.37	1537.82	875.22	2591.18	741.89	123.58
241	LSG	3	6919.50	121855.56	4350.94	9963.64	137274.67	259622.04	26846.07	88929.05	11329.31	7322.41	36108.53	1754.60	412.96	2676.13	1054.78	63.09

Appendix B

Monazite Elemental Concentrations

In ppm measured with

Cameca SX-50 at UTK

Table 1. Monazite element concentrations in parts per million as measured by Cameca SX-50

Analysis	sample	grain	P	Si	Th	Y	La	Ce	Pr	Nd	Gd	Dy	U	Ca	Fe	Sm	Pb
#1	XG-4	4	114601.66	15206.75	85073.04	4078.94	77150.06	206045.51	25232.33	116110.46	10541.17	2361.26	4010.49	5538.60	0.00	20110.09	8141.33
#2	XG-4	4	129452.74	1252.82	20368.41	20434.06	111905.11	239061.63	25702.29	101124.04	18609.72	9131.37	5720.45	5252.73	0.00	17410.92	3991.76
#3	XG-4	4	124521.29	5058.01	41067.88	4086.81	95960.08	238831.11	28299.86	120774.42	12788.22	3006.03	3605.03	5181.27	0.00	21438.11	5347.10
#4	XG-4	11	117438.33	12257.02	79276.71	3323.00	71880.53	204346.47	28504.93	125309.79	9881.81	2230.56	4768.51	6803.54	46.64	20791.35	9422.40
#5	XG-4	11	130028.80	766.65	21596.30	26103.63	107172.76	227552.52	25488.67	97411.73	19989.19	10115.95	11026.63	6917.89	0.00	17186.71	5987.63
#6	XG-4	3	113248.78	11551.14	82117.70	3299.37	68529.52	205157.57	27983.71	126252.87	10463.09	2387.40	4028.11	7339.53	0.00	22015.89	8791.15
#7	XG-4	3	126694.62	1631.46	23684.90	19906.48	108716.10	236047.75	25454.49	103524.61	18297.39	8242.63	6249.31	5538.60	0.00	17152.22	4706.56
#8	XG-4	6	108186.41	16870.93	105224.77	1866.23	67156.71	195415.81	26086.80	119008.29	8363.53	2082.44	3684.36	6889.30	108.82	18626.84	11409.00
#9	XG-4	6	128043.13	2440.18	25412.37	10157.97	106183.66	242331.66	26787.46	112638.20	18071.82	5532.84	4239.66	5224.15	0.00	18989.03	5309.96
#10	XG-4	6	122880.38	2141.01	26080.48	10559.57	101204.03	235330.56	28248.59	113787.05	20258.14	5489.28	5958.43	5602.92	77.73	21326.01	5477.06
#11	XG-4	11	125429.03	3749.10	38431.54	8882.32	93129.20	228986.89	25950.08	114875.88	18306.07	4347.86	6557.80	6639.17	0.00	21101.80	6331.11
#12	XG-4	10	126646.61	3361.10	29625.69	6173.53	103949.65	245772.44	28069.15	116427.67	16119.75	3668.23	3322.97	4373.70	0.00	21386.37	3369.78
#13	XG-4	10	126930.28	3435.89	30540.58	11110.78	99601.00	235501.32	26522.57	113075.45	18939.41	5916.22	4415.94	4723.89	0.00	20411.91	5337.81
#14	XG-4	10	130264.47	1566.02	23763.15	24072.04	104060.50	227987.96	25719.38	101132.61	20752.66	9819.71	7227.69	5695.82	0.00	18445.75	5003.62
#15	XG-4	17	123543.73	3333.05	42265.66	7842.90	95380.26	231377.51	27001.07	111935.18	14627.50	4077.75	7113.10	8082.78	46.64	20420.54	7101.61
#16	XG-4	17	122343.60	1173.35	21812.98	23418.46	105390.67	224154.43	24446.22	100275.26	23511.59	11335.79	6778.16	5767.29	0.00	18652.71	4381.65
#17	XG-6	8	110237.54	13692.15	77537.21	0.00	84926.46	234007.19	29256.86	120191.43	1709.14	496.65	1419.09	3544.70	0.00	11443.43	9255.30
#18	XG-6	8	120440.84	5530.15	38672.30	196.86	103020.23	256146.00	29530.29	121674.64	5257.57	827.75	916.68	3787.69	0.00	15530.99	5003.62
#19	XG-6	8	122788.74	2963.75	33826.98	2716.67	110464.09	245447.99	26223.51	108068.54	14549.42	2866.62	2802.93	5803.02	0.00	19058.02	4734.41
#20	XG-6	23	3709.50	87304.39	458451.85	6244.40	51.16	640.34	0.00	1200.29	4199.12	4513.40	31801.82	0.00	202.10	1086.57	0.00
#21	XG-6	23	121339.85	5450.68	33881.15	1456.76	113499.61	257640.14	29342.30	115510.31	9821.08	1455.09	431.90	1665.15	0.00	17117.72	1086.13
#22	XG-6	23	126022.55	2496.28	105868.81	7197.20	95806.60	190574.81	20020.10	75763.72	5925.61	2361.26	2344.59	22347.34	0.00	9339.29	0.00
#23	XG-6	19	123622.28	1757.68	30197.50	7275.94	108767.26	242784.16	26334.59	106113.79	17716.11	4225.87	2635.46	6531.97	0.00	19618.55	3871.08
#24	XG-6	19	114610.39	11495.05	66516.36	0.00	90196.00	244141.69	30025.88	122300.50	2524.68	1123.99	1013.64	3201.67	0.00	10555.21	7537.92
#25	XG-6	19	123233.88	3506.01	31136.47	2000.10	113422.87	254395.73	28428.03	112509.60	11937.99	2143.43	2080.16	4044.96	0.00	17600.64	4270.25
#26	XG-5	9	118795.57	3183.46	34573.34	10291.84	113388.76	242528.03	25932.99	90270.03	11018.34	3973.19	11291.06	6724.93	0.00	14892.85	6331.11
#27	XG-5	9	121566.78	3174.11	31678.18	9126.43	117114.96	247462.94	25685.20	91641.78	11747.12	3746.65	10286.23	6524.82	0.00	17729.99	5894.80
#28	XG-5	11	127192.13	3664.95	27765.81	2385.94	121540.34	268252.77	26881.45	102418.63	7096.86	1263.40	3490.44	3880.59	0.00	12228.18	3991.76
#29	XG-5	11	121523.14	5801.28	43403.26	3574.98	120150.48	254344.50	26565.30	97103.08	8467.64	2213.14	863.80	4330.83	0.00	12081.58	4186.70
#30	XG-5	11	124303.08	3206.83	38479.69	3763.96	117183.17	251595.29	25505.76	98089.03	12276.34	3258.71	2282.89	6603.44	0.00	14763.50	4270.25
#31	XG-5	5	114610.39	8152.65	52889.26	3779.71	116390.18	253524.86	24873.46	93579.39	6498.22	2247.99	2212.38	3737.66	77.73	10236.14	5142.87
#32	XG-5	5	121488.23	3534.06	41519.30	4693.14	112442.29	245465.07	25497.21	100472.45	11825.20	2788.20	2776.49	6889.30	69.96	15772.45	4437.35

Table 1. Monazite element concentrations in parts per million as measured by Cameca SX-50

Analysis	sample	grain	P	Si	Th	Y	La	Ce	Pr	Nd	Gd	Dy	U	Ca	Fe	Sm	Pb
#1	XG-4	4	114601.66	15206.75	85073.04	4078.94	77150.06	206045.51	25232.33	116110.46	10541.17	2361.26	4010.49	5538.60	0.00	20110.09	8141.33
#2	XG-4	4	129452.74	1252.82	20368.41	20434.06	111905.11	239061.63	25702.29	101124.04	18609.72	9131.37	5720.45	5252.73	0.00	17410.92	3991.76
#3	XG-4	4	124521.29	5058.01	41067.88	4086.81	95960.08	238831.11	28299.86	120774.42	12788.22	3006.03	3605.03	5181.27	0.00	21438.11	5347.10
#4	XG-4	11	117438.33	12257.02	79276.71	3323.00	71880.53	204346.47	28504.93	125309.79	9881.81	2230.56	4768.51	6803.54	46.64	20791.35	9422.40
#5	XG-4	11	130028.80	766.65	21596.30	26103.63	107172.76	227552.52	25488.67	97411.73	19989.19	10115.95	11026.63	6917.89	0.00	17186.71	5987.63
#6	XG-4	3	113248.78	11551.14	82117.70	3299.37	68529.52	205157.57	27983.71	126252.87	10463.09	2387.40	4028.11	7339.53	0.00	22015.89	8791.15
#7	XG-4	3	126694.62	1631.46	23684.90	19906.48	108716.10	236047.75	25454.49	103524.61	18297.39	8242.63	6249.31	5538.60	0.00	17152.22	4706.56
#8	XG-4	6	108186.41	16870.93	105224.77	1866.23	67156.71	195415.81	26086.80	119008.29	8363.53	2082.44	3684.36	6889.30	108.82	18626.84	11409.00
#9	XG-4	6	128043.13	2440.18	25412.37	10157.97	106183.66	242331.66	26787.46	112638.20	18071.82	5532.84	4239.66	5224.15	0.00	18989.03	5309.96
#10	XG-4	6	122880.38	2141.01	26080.48	10559.57	101204.03	235330.56	28248.59	113787.05	20258.14	5489.28	5958.43	5602.92	77.73	21326.01	5477.06
#11	XG-4	11	125429.03	3749.10	38431.54	8882.32	93129.20	228986.89	25950.08	114875.88	18306.07	4347.86	6557.80	6639.17	0.00	21101.80	6331.11
#12	XG-4	10	126646.61	3361.10	29625.69	6173.53	103949.65	245772.44	28069.15	116427.67	16119.75	3668.23	3322.97	4373.70	0.00	21386.37	3369.78
#13	XG-4	10	126930.28	3435.89	30540.58	11110.78	99601.00	235501.32	26522.57	113075.45	18939.41	5916.22	4415.94	4723.89	0.00	20411.91	5337.81
#14	XG-4	10	130264.47	1566.02	23763.15	24072.04	104060.50	227987.96	25719.38	101132.61	20752.66	9819.71	7227.69	5695.82	0.00	18445.75	5003.62
#15	XG-4	17	123543.73	3333.05	42265.66	7842.90	95380.26	231377.51	27001.07	111935.18	14627.50	4077.75	7113.10	8082.78	46.64	20420.54	7101.61
#16	XG-4	17	122343.60	1173.35	21812.98	23418.46	105390.67	224154.43	24446.22	100275.26	23511.59	11335.79	6778.16	5767.29	0.00	18652.71	4381.65
#17	XG-6	8	110237.54	13692.15	77537.21	0.00	84926.46	234007.19	29256.86	120191.43	1709.14	496.65	1419.09	3544.70	0.00	11443.43	9255.30
#18	XG-6	8	120440.84	5530.15	38672.30	196.86	103020.23	256146.00	29530.29	121674.64	5257.57	827.75	916.68	3787.69	0.00	15530.99	5003.62
#19	XG-6	8	122788.74	2963.75	33826.98	2716.67	110464.09	245447.99	26223.51	108068.54	14549.42	2866.62	2802.93	5803.02	0.00	19058.02	4734.41
#20	XG-6	23	3709.50	87304.39	458451.85	6244.40	51.16	640.34	0.00	1200.29	4199.12	4513.40	31801.82	0.00	202.10	1086.57	0.00
#21	XG-6	23	121339.85	5450.68	33881.15	1456.76	113499.61	257640.14	29342.30	115510.31	9821.08	1455.09	431.90	1665.15	0.00	17117.72	1086.13
#22	XG-6	23	126022.55	2496.28	105868.81	7197.20	95806.60	190574.81	20020.10	75763.72	5925.61	2361.26	2344.59	22347.34	0.00	9339.29	0.00
#23	XG-6	19	123622.28	1757.68	30197.50	7275.94	108767.26	242784.16	26334.59	106113.79	17716.11	4225.87	2635.46	6531.97	0.00	19618.55	3871.08
#24	XG-6	19	114610.39	11495.05	66516.36	0.00	90196.00	244141.69	30025.88	122300.50	2524.68	1123.99	1013.64	3201.67	0.00	10555.21	7537.92
#25	XG-6	19	123233.88	3506.01	31136.47	2000.10	113422.87	254395.73	28428.03	112509.60	11937.99	2143.43	2080.16	4044.96	0.00	17600.64	4270.25
#26	XG-5	9	118795.57	3183.46	34573.34	10291.84	113388.76	242528.03	25932.99	90270.03	11018.34	3973.19	11291.06	6724.93	0.00	14892.85	6331.11
#27	XG-5	9	121566.78	3174.11	31678.18	9126.43	117114.96	247462.94	25685.20	91641.78	11747.12	3746.65	10286.23	6524.82	0.00	17729.99	5894.80
#28	XG-5	11	127192.13	3664.95	27765.81	2385.94	121540.34	268252.77	26881.45	102418.63	7096.86	1263.40	3490.44	3880.59	0.00	12228.18	3991.76
#29	XG-5	11	121523.14	5801.28	43403.26	3574.98	120150.48	254344.50	26565.30	97103.08	8467.64	2213.14	863.80	4330.83	0.00	12081.58	4186.70
#30	XG-5	11	124303.08	3206.83	38479.69	3763.96	117183.17	251595.29	25505.76	98089.03	12276.34	3258.71	2282.89	6603.44	0.00	14763.50	4270.25
#31	XG-5	5	114610.39	8152.65	52889.26	3779.71	116390.18	253524.86	24873.46	93579.39	6498.22	2247.99	2212.38	3737.66	77.73	10236.14	5142.87
#32	XG-5	5	121488.23	3534.06	41519.30	4693.14	112442.29	245465.07	25497.21	100472.45	11825.20	2788.20	2776.49	6889.30	69.96	15772.45	4437.35

Table 1. Monazite element concentrations in parts per million as measured by Cameca SX-50

Analysis	sample	grain	P	Si	Th	Y	La	Ce	Pr	Nd	Gd	Dy	U	Ca	Fe	Sm	Pb
#33	XG-5	5	128937.77	1753.01	34838.18	11874.59	116475.45	238984.79	23301.24	93647.97	15503.77	6526.14	6046.58	8018.46	0.00	15211.92	4409.50
#34	XG-7	1	122958.94	3772.47	12609.88	3283.62	150249.92	294839.84	24796.55	81988.06	4060.30	1228.55	237.98	4287.95	0.00	6036.48	659.10
#35	XG-7	1	119188.34	4941.14	20434.62	3811.21	140068.98	287838.74	26120.97	86369.10	3548.43	1498.66	264.43	4981.16	0.00	8200.98	0.00
#36	XG12	1	124547.48	1986.74	42723.11	17126.82	109585.83	236013.60	26420.04	97934.71	11755.79	4870.64	1075.34	7968.43	0.00	13720.05	0.00
#37	XG-12	1	122740.73	3594.83	42187.42	1960.73	113414.34	249477.89	25975.71	106010.91	8779.97	1028.15	2503.25	6746.37	0.00	14780.74	4845.81
#38	XG12	1	87496.14	162552.78	31636.05	653.58	83613.34	185469.14	18789.67	76698.23	6246.62	731.90	1674.71	4931.14	15.55	10693.19	5282.11
#39	XG12	1	112419.60	9167.05	108800.08	9118.55	91150.99	196841.64	21224.89	80487.70	7799.60	3598.53	8073.86	15636.71	77.73	10555.21	621.97
#40	XG12	14	126786.27	1594.07	35626.67	25087.83	109321.50	235100.04	24335.14	97420.30	13864.03	7284.18	1260.44	7082.26	0.00	13383.73	668.39
#41	XG12	14	123063.68	3520.04	44516.78	1110.29	107624.68	247684.93	27274.50	108763.00	9100.98	1542.23	2124.23	7468.17	101.05	16048.40	3908.21
#42	XG12	17	123757.57	3763.12	39767.77	1771.74	114582.51	250246.30	25428.86	105676.55	9352.58	1812.33	2212.38	6353.31	0.00	15168.80	4938.64
#43	XG12	17	121182.74	5656.37	58276.30	1165.41	92668.75	234314.55	27855.54	116393.38	6888.63	810.32	2371.03	8725.97	256.51	15772.45	5931.94
#44	XG12	17	127733.28	1477.20	39430.70	20347.45	110634.62	235851.38	24446.22	96494.37	11165.83	6360.59	2591.39	8354.35	0.00	12512.75	83.55
#45	XG12	17	119105.42	3894.01	53280.50	15307.83	99771.54	231719.03	24591.48	103798.96	10150.76	4530.83	1621.82	7846.94	0.00	14513.41	1234.66
#46	XG12	20	126376.04	1308.91	39563.12	18473.34	108110.70	235390.33	25403.22	96374.34	11885.93	5071.05	2943.96	8897.49	0.00	14323.70	0.00
#47	XG12	20	120266.28	2790.79	36397.11	2511.93	119152.85	250382.91	26821.63	101072.60	10176.79	2056.30	3393.49	6210.37	0.00	14202.97	4195.99
#48	XG12	13	129142.89	635.76	25376.25	22355.42	114505.77	246028.57	24215.52	99306.46	13117.90	7240.62	793.28	5817.31	0.00	13875.27	1160.39
#49	XG12	13	122889.11	3375.12	43469.47	5921.55	114360.81	245499.22	25240.88	99409.34	10358.98	1969.17	2300.52	7125.14	23.32	14539.28	4743.69
#50	XG-10	6	115587.95	7133.57	46858.19	685.07	107658.79	255556.89	28282.77	114112.84	5509.17	1167.56	872.61	3401.77	31.09	12650.73	6229.00
#51	XG-10	6	118930.86	3641.58	29258.53	2637.92	116842.10	256359.45	27453.94	104647.73	14367.23	2518.10	3137.87	4030.67	0.00	17488.53	3109.86
#52	XG-10	6	115718.87	7301.86	48633.80	811.06	106584.42	258348.78	28180.23	111900.88	4572.18	1315.68	1595.38	3351.74	0.00	12823.20	3574.01
#53	XG-10	15	117473.24	6998.00	45624.29	622.08	108281.24	256359.45	27915.35	113718.46	5639.31	880.03	793.28	3416.06	46.64	13452.72	7222.29
#54	XG-10	15	119389.09	4300.71	32292.12	1700.87	116782.41	259296.49	28564.74	108385.76	9604.18	1725.20	590.55	3301.72	0.00	16126.02	4233.12
#55	XG-10	30	118254.42	5632.99	34597.41	1653.62	114113.54	258280.48	27283.05	111120.70	8398.23	1428.95	2106.61	2365.52	38.87	14806.61	4131.00
#56	XG-10	30	123940.86	2052.19	31268.89	12291.94	112459.35	238643.28	26437.13	98654.88	18227.99	5750.67	5746.89	6660.61	0.00	16186.38	3592.58
#57	XG-9	22	99362.17	16412.81	122108.17	1007.92	68435.72	189499.03	23959.18	104296.22	7582.70	1289.54	3014.47	10512.61	248.74	16833.15	11761.76
#58	XG-9	22	111808.62	7184.99	71879.32	1504.01	79895.68	216521.54	27479.57	120362.90	7634.76	1577.08	4169.14	9876.57	0.00	18920.04	8614.77
#59	XG-9	22	125690.87	462.79	22860.30	10016.24	113934.48	242425.57	25309.23	101209.77	16241.21	5855.23	6831.05	6789.25	0.00	15841.44	4520.90
#60	XG-9	6	106506.22	15875.23	120272.36	779.57	69663.57	189789.32	24147.16	107296.93	6220.59	1010.72	3975.23	10777.04	0.00	15418.89	11344.01
#61	XG-9	6	127768.19	719.90	27248.17	8551.60	115520.45	246549.39	25488.67	102170.00	16111.08	5768.10	7941.64	7825.50	0.00	16565.82	4706.56
#62	XG-9	6	126886.64	1846.50	35265.53	3519.86	111708.99	248829.01	26548.21	105153.57	12632.06	2491.96	3657.91	7575.37	0.00	17247.08	4920.07
#63	IG-1	2	127453.98	1023.76	10208.28	6323.14	153984.64	281964.66	25454.49	85743.24	5951.64	2326.41	61.70	4480.90	0.00	10098.16	0.00
#64	IG-1	2	124975.16	1762.36	21800.95	9811.50	130297.32	262096.93	26026.98	94128.09	8701.89	3607.24	229.17	6524.82	31.09	13288.87	0.00

Table 1. Monazite element concentrations in parts per million as measured by Cameca SX-50

Analysis	sample	grain	P	Si	Th	Y	La	Ce	Pr	Nd	Gd	Dy	U	Ca	Fe	Sm	Pb
#20	IG-4	1	123294.97	6843.74	74467.50	18536.33	98509.58	206771.24	22147.71	88812.54	16258.57	7266.76	2776.49	11341.62	0.00	17505.78	0.00
#21	IG-4	7	117818.01	34545.91	63717.51	23599.57	61546.10	178468.05	24266.79	115055.92	23303.37	8721.85	2027.28	5824.46	77.73	26569.12	816.92
#22	IG-4	7	129897.88	2033.49	30149.35	21827.83	100496.31	231710.49	25591.21	108557.23	18731.19	7528.15	819.73	7532.49	0.00	20618.88	0.00
#23	IG-4	7	131268.21	1028.43	22246.35	15992.90	111325.29	245755.36	27265.96	106868.26	17429.81	6473.86	564.11	4380.85	0.00	21567.47	269.21
#24	IG-4	10	119428.37	9653.22	75857.90	24599.62	62015.08	182002.74	25181.06	121040.20	27485.13	9967.83	1198.74	5588.62	0.00	27138.27	0.00
#25	IG-4	10	126236.39	4599.89	33724.65	20489.19	87782.92	227065.86	27505.21	125395.52	20813.39	7362.60	308.50	3651.90	0.00	23619.87	0.00
#26	IG-4	10	130295.01	1079.85	15866.18	22394.79	115068.53	248205.74	25753.55	103704.65	16475.46	7136.06	52.89	6632.02	0.00	17548.90	176.38
#27	IG-4	21	47451.02	4118.40	23311.72	7874.40	20455.68	60943.64	8852.25	40466.76	7348.46	2439.68	414.27	2043.92	93.28	9434.15	0.00
#28	IG-4	21	130556.86	1879.22	30275.75	21867.21	102210.19	231283.59	26385.86	107939.94	17933.01	7510.72	793.28	7746.89	0.00	19627.17	269.21
#29	IG-4	21	132306.87	388.00	24190.50	20646.67	110651.68	233076.55	26180.79	103730.37	19659.50	7702.41	3975.23	8511.57	0.00	20601.63	389.89
#30	IG-4	25	122365.42	6689.47	49638.98	22237.30	74660.25	210399.85	27727.37	126115.69	21507.46	7876.68	899.05	4330.83	0.00	24663.32	0.00
#31	IG-4	25	128344.26	2594.45	34422.86	20859.28	97298.78	228628.30	26787.46	112689.64	18765.89	7109.92	449.53	8054.19	0.00	19765.15	761.22
#32	IG-4	23	125603.59	5254.34	47490.19	24229.53	77653.14	205678.38	27026.71	121614.62	26513.43	9567.02	1419.09	4873.97	0.00	26569.12	0.00
#33	IG-4	23	129269.45	1954.02	35891.51	19922.23	99021.19	228978.36	25283.60	107588.43	18601.05	7127.35	1965.58	8840.31	0.00	20662.00	0.00
#34	IG-4	23	125978.90	4819.60	38407.46	21780.59	90818.45	223642.16	26385.86	120843.01	21325.27	7841.82	405.46	3401.77	0.00	23576.75	0.00
#35	IG-3	6	130644.14	752.62	13193.73	7622.42	146046.23	268167.39	24788.01	90853.02	6446.17	2701.07	343.76	8776.00	155.46	10546.59	0.00
#36	IG-3	6	131041.28	1033.11	21806.96	8488.60	132369.32	262190.85	27582.11	96785.86	8901.43	3232.57	202.73	6817.83	0.00	10805.29	761.22
#37	IG-3	6	129836.78	1154.65	26152.71	8669.71	130169.41	258237.79	25061.44	97737.52	8806.00	3554.96	343.76	7017.94	0.00	12072.95	0.00
#38	IG-3	6	129483.29	1154.65	25502.65	9370.53	125223.90	248248.43	25582.66	92653.45	8276.77	3703.08	766.84	7282.36	0.00	11797.00	0.00
#39	IG-3	7	132075.57	757.30	25755.45	19205.66	108051.02	244517.36	25591.21	102470.07	17169.53	6648.12	520.04	5531.45	0.00	20006.61	0.00
#40	IG-3	7	130766.34	771.32	22222.28	12323.43	128097.41	255104.38	24147.16	97780.39	10254.87	4443.70	564.11	7618.25	0.00	13245.75	213.51
#41	IG-3	7	131490.78	1023.76	25291.99	8795.70	129649.28	260560.10	24471.86	99169.29	8467.64	3485.25	414.27	5595.77	147.69	13582.07	0.00
#42	IG-3	20	132734.55	780.67	21548.15	15740.92	122512.39	253234.57	26445.67	98654.88	13586.40	5410.86	0.00	5259.88	0.00	16824.52	259.93
#43	IG-3	20	130962.72	785.35	15655.51	8992.56	139011.66	265862.15	25557.03	95757.05	8571.75	3241.29	237.98	8097.07	0.00	11719.39	0.00
#44	IG-3	20	129714.59	1958.69	31064.24	20536.43	112715.15	239701.98	25659.56	101158.33	13490.97	6334.45	308.50	8018.46	0.00	14211.59	0.00
#45	IG-3	20	129797.51	1327.61	16323.62	18591.46	122938.73	252867.44	28368.21	101861.36	11434.79	5166.89	396.64	7511.05	0.00	13814.91	956.16
#46	IG-3	20	132241.41	724.58	27212.06	18685.95	107829.32	242066.98	27197.60	102864.45	16848.52	6839.81	1207.55	6324.72	0.00	20946.57	0.00
#47	IG-3	20	130892.90	1771.71	24726.20	8803.58	132224.36	264350.94	26368.77	99683.69	10376.33	3154.16	0.00	4495.20	0.00	12530.00	0.00
#48	IG-3	20	130168.46	1617.44	23835.38	8228.75	131115.88	263488.61	26531.12	100429.59	10003.27	3232.57	881.43	4416.58	0.00	13185.39	0.00
#49	IG-3	27	129954.61	1598.74	25201.70	26268.99	109278.87	238455.44	25565.57	101501.27	14653.53	6979.22	564.11	9383.45	0.00	14642.77	640.54
#50	IG-3	27	129221.44	1636.14	26435.60	25505.18	110250.92	237516.27	24907.63	100352.43	13577.72	7623.99	951.94	9247.67	0.00	14366.81	9.28
#51	IG-3	27	130260.10	2159.70	23305.70	8606.72	119783.83	257802.36	27889.71	105307.89	14054.90	5140.75	696.33	3673.34	0.00	19885.88	46.42

REFERENCES

Ayers J. C. (1991) Experimental studies of the chemistry of aqueous fluid-accessory mineral systems at high P-T conditions with implications for fluid-rock interactions. Ph.D., Rensselaer Polytechnic Institute.

Ayers J. C., Miller C., Gorisch B., and Milleman J. (1999) Textural development of monazite during high-grade metamorphism; hydrothermal growth kinetics, with implications for U, Th-Pb geochronology. *American Mineralogist* **84**(11-12), 1766-1780.

Bachl, A.C., Miller, C.F., Miller, J.S., Faulds, J.E. (2001) Construction of a pluton: Evidence from an exposed cross section of the Searchlight pluton, Eldorado Mountains, Nevada: GSA Bulletin, **113**, 9, 1213 – 1228.

Bennett V. C. and DePaolo D. J. (1987) Proterozoic crustal history of the Western United States as determined by neodymium isotopic mapping; with Suppl. Data 87-30. *Geol Soc Am Bull* **99**(5), 674-685.

Braun I., Montel J. M., and Nicollet C. (1998) Electron microprobe dating of monazites from high-grade gneisses and pegmatites of the Kerala Khondalite Belt, southern India. *Chem. Geol.* **146**, 65-85.

Cates, N.L., Miller, J.S., Miller, C.F., Wooden, J.L., Ericksen, S., Means, M. (2003) Longevity of plutonic systems: Shrimp evidence from Aztec Wash and searchlight plutons, Nevada, Abstracts with programs

Catlos, E.J., Gilley, L.D., Harrison, T.M. (2002) Interpretation of monazite ages via in situ analysis, Chemical Geology, v. 188; p. 193-215.

Catlos, E.J., Cemen, I., 2005, Monazite ages and the evolution of the Menderes Massif, western Turkey, International Journal of Earth Science, v. 94; p. 204-217.

Cetiner Z. S., Wood S. A., and Gammons C. H. (2005) The aqueous geochemistry of the rare earth elements. Part XIV. The solubility of rare earth element phosphates from 23 to 150 [deg]C. *Chemical Geology* **217**(1-2), 147-169.

Falkner, C.M., Miller, C.F., Wooden, J.L., and Heizler, M.T. (1995) Petrogenesis and tectonic significance of the calc-alkaline, bimodal Aztec Wash pluton, Eldorado Mountains, Colorado River extensional corridor. Journal of Geophysics Research, v. 100 p. 204-227.

Faulds, J.E., Geissman, J.W., and Mawer, C.K. (1990) Structural development of a major extensional accommodation zone in the Basin and Range Province, northwestern Arizona and southern Nevada: implications for kinematic models of continental extension. Geologic Society of America Memoirs, v. 176, p. 37-76.

Hammond J. G. and Wooden J. L. (1990) Isotopic constraints on the petrogenesis of Proterozoic diabase in southwestern USA. *Proceedings of the International Dyke Conference* **2**, 145-156.

Kapp, J., Miller, C.F., Miller, J.S. (2002) Ireteba Pluton, Eldorado Mountains, Nevada: Late, Deep-Source, Peraluminous Magmatism in the Cordilleran Interior, The Journal of Geology, v. 110; p. 649-669.

Loflin M. I. (2002) Monazite as a Tracer of Fluid Infiltration Associated with Contact Metamorphism. M.Sc., Vanderbilt University.

Ludwig K. R. (2001) Users Manual for Isoplot/Ex: A Geochronological Toolkit for Microsoft Excel. In *Berkeley Geochronology Center Special Publication*, pp. 53.

McFarlane, C.R.M., Connelly, J.N., Carlson, W.D. (2005) Monazite and xenotime petrogenesis in the contact aureole of the Makhavinekh Lake Pluton, northern Labrador; Contributions to Mineralogy and Petrology, v. 148; p. 524-541.

Means, M.A., Miller, J.S., Miller, C.F., Cates, N.L., Wooden, J.L., Koteas, C., (2003) Mafic injection and local hybridization in a nearly frozen magma chamber: failed (?) rejuvenation in the Searchlight pluton, Eldorado Mountains, Nevada (USA), Abstract with programs

Miller C. F., Wooden, J.L.,. (1994) Anatexis, hybridization and the modification of ancient crust: Mesozoic plutonism in the Old Woman Mountains area, California. *Lithos* **32**, 111-133.

Miller, J.S., Cates, N.L., Miller, C.F., Wooden, J.L., Means, M.A., Ericksen, S. (2003) Magmatic construction and duration of solidification of Searchlight pluton, Eldorado Mountains, Nevada (USA), Abstracts with programs

Montel, J.M., Foret, S., Veschambre, M., Nicollet, C., Provost, A. (1996) Electron microprobe dating of monazite, Chemical Geology, v. 131; p. 37-53.

Patrick D. W., Miller, C.F. (1997) Processes in a composite, recharging magma chamber: evidence from magmatic structures in the Aztec Wash Pluton, Nevada. *(B) Proc. 30th Intl. Geol. Congr.*, 121-135.

Pyle J. M. and Spear F. S. (2003) Four generations of accessory-phase growth in low-pressure migmatites from SW New Hampshire. *American Mineralogist* **88**(2-3), 338-351.

Seydoux-Guillaume, A. M., Writh, R., Nasdala, L., Gottschalk, M., Montel, J.M., Heinrich, W. (2002) An XRD, TEM and Raman study of experimentally annealed natural monazite, Physical Chemistry Minerals, v. 29; 240-253.

Seydoux-Guillaume, A. M., Paquette, J., Wiedenbeck, M., Montel, J., Heinrich, W. (2002) Experimental resetting of the U-Th-Pb systems in monazite, Chemical Geology, v. 191; 165-181.

Spear, F.S., and Pyle, J.M. (2002) Apatite, Monazite, and Xenotime in metamorphic rocks.In M.J. importance, 48, p. 293-335. Mineralogical Society of America.

Taylor S. R. and McLennan S. M. (1985) *The Continental Crust: Its Composition and Evolution.* Blackwell.

Townsend, K.J., Miller, C.F., D'Andrea, J.L., Ayers, J.C., Harrison, T.M., Coath, C.D. (2000) Low temperature replacement of monazite in the Ireteba granite, Southern Nevada: geochronological implications: Chemical Geology, v. 172; p. 95 – 112.

Winter, John D., (2001) An Introduction To Igneous And Metamorphic Petrology. Prentice Hall. Upper Saddle River, New Jersey. 697 p.

Wood S. A. and Williams-Jones A. E. (1994) The aqueous geochemistry of the rare earth elements and yttrium 4. Monazite solubility and REE mobility in exhalative massive-sufide-depositing environments. *Chem. Geol.* **115**, 47-60.

Wooden J. L. and Miller D. M. (1990) Chronologic and isotopic framework for early Proterozoic crustal evolution in the eastern Mojave Desert region, SE California. *Journal of Geophysical Research* **95**(B12), 20,133-20,146.